CANADIAN THESES ON MICROFICHE

THÈSES CANADIENNES SUR MICROFICHE

National Library of Canada
Collections Development Branch

Canadian Theses on
Microfiche Service

Ottawa, Canada
K1A 0N4

Bibliothèque nationale du Canada
Direction du développement des collections

Service des thèses canadiennes
sur microfiche

NOTICE

The quality of this microfiche is heavily dependent upon the quality of the original thesis submitted for microfilming. Every effort has been made to ensure the highest quality of reproduction possible.

If pages are missing, contact the university which granted the degree.

Some pages may have indistinct print especially if the original pages were typed with a poor typewriter ribbon or if the university sent us an inferior photocopy.

Previously copyrighted materials (journal articles, published tests, etc.) are not filmed.

Reproduction in full or in part of this film is governed by the Canadian Copyright Act, R.S.C. 1970, c. C-30. Please read the authorization forms which accompany this thesis.

AVIS

La qualité de cette microfiche dépend grandement de la qualité de la thèse soumise au microfilmage. Nous avons tout fait pour assurer une qualité supérieure de reproduction.

S'il manque des pages, veuillez communiquer avec l'université qui a conféré le grade.

La qualité d'impression de certaines pages peut laisser à désirer, surtout si les pages originales ont été dactylographiées à l'aide d'un ruban usé ou si l'université nous a fait parvenir une photocopie de qualité inférieure.

Les documents qui font déjà l'objet d'un droit d'auteur (articles de revue, examens publiés, etc.) ne sont pas microfilmés.

La reproduction, même partielle, de ce microfilm est soumise à la Loi canadienne sur le droit d'auteur, SRC 1970, c. C-30. Veuillez prendre connaissance des formules d'autorisation qui accompagnent cette thèse.

THIS DISSERTATION
HAS BEEN MICROFILMED
EXACTLY AS RECEIVED

LA THÈSE A ÉTÉ
MICROFILMÉE TELLE QUE
NOUS L'AVONS REÇUE

Canada

NL 339 (r. 85/09)

COMPARISON OF THE RNA GENOMES OF PERSISTENT AND PARENTAL STRAINS OF HUMAN CORONAVIRUS 229E

A Thesis submitted to the

School of Graduate Studies

University of Ottawa

In Partial Fulfilment of the

Requirements for the Degree of

Master of Science

Department of Microbiology and Immunology

School of Medicine

By

Donald Angus McLeod

Ottawa

Ontario

Canada

May 1985

ABSTRACT

Coronaviruses can cause in vivo and in vitro persistent infections. In 1978, an in vitro persistent infection with the human coronavirus strain 229E was established in L132 cells. A number of biological differences were observed between the parental 229E virus and the persistent VH virus derived from it. These differences made it of interest to study the RNA genomes of these two viruses.

A number of molecular differences have been found between the 229E RNA and the VH RNA genomes. By agarose gel electrophoresis, the 60S genomic RNA of parental 229E virus migrated faster than the 60S genomic RNA of persistent VH virus. This indicated that the VH RNA was larger than the 229E RNA.

In liquid hybridization experiments, a 2 log difference in the 50% R_0t values was found using a cDNA probe synthesized with random primers and 229E RNA template. When hybridized to completion under these conditions, VH RNA was saturated at 67% of the value for 229E RNA. This represents a 33% difference between the 229E RNA and the VH RNA.

Northern blot hybridization revealed a pattern of preferential hybridization for 229E RNA when random primed cDNA was used. Northern blots using a cDNA probe synthesized from oligo-dT primers, representing only the 3'-end of the genome, did not reveal these differences so strongly. This implied that any changes in the RNA genome were not at the 3'-end.

These facts, when taken together, indicated that there were molecular differences between the RNA genomes of the parental human coronavirus 229E and the persistent VH strain derived from it, and that these differences were probably upstream from the 3'-end of the genome.

ACKNOWLEDGEMENTS

I would like to acknowledge the advice, support and assistance that I received from my supervisors, colleagues, associates and fellow students.

Dr. C.M. Johnson-Lussenburg, my supervisor for allowing me the opportunity to study in her laboratory.

Dr. T. Chudzio for advice and assistance on problems encountered in the laboratory.

Mr. A. Brunner for helping with cell cultures, plaque assays and photography.

A special thanks to Dr. M.P.R. Tenniswood, who gave so unstintingly of his knowledge in molecular biology and also for complete access to his resources, laboratory and equipment.

Dedicated to Filomena and Michael

TABLE OF CONTENTS

LIST OF ABBREVIATIONS

Act-D	actinomycin-D
BCV	bovine coronavirus
BUDR	bromo-deoxyuridine
cDNA-rep.	complementary deoxyribonucleic acid-representative (synthesized with random primers)
cDNA-3'	complementary deoxyribonucleic acid-3' (synthesized with oligo-dT primer)
CCV	canine coronavirus
cm^2	square centimetres
DEAE	di-ethyl-amino-ethyl
E1	matrix protein
E2	peplomer protein
g/L	grams per litre
g/mL	grams per millilitre
HCV	human coronavirus
HCV 229E	human coronavirus strain 229E
HEV	human enteric coronavirus
HV-1	L132 cells persistently infected with HCV 229E
IBV	infectious bronchitis virus
i.c.	intra-cerebral
MEM	minimum essential medium
MHV	murine hepatitis virus
mM	millimolar
mRNA	messenger RNA
N	non-glycosylated nucleoprotein
$NaHCO_3$	sodium bicarbonate

nm	nanometer
pfu	plaque forming unit
PPO	diphenyl oxazole
RNA	ribonucleic acid
RNP	ribonucleoprotein
SNF	supernatant fluid
TCV	turkey coronavirus
TGEV	transmissible gastro-enteritis virus
ug	microgram
VH	persistent strain of HCV 229E
xg	centrifugal force expressed in gravitational units

LIST OF TABLES

LIST OF FIGURES

I. LITERATURE REVIEW

The coronaviruses have been classified as a separate group of viruses since 1968 (Tyrrell, Almeida, Berry, Cunningham, Hamre, Hofstad, Malluci, and MacIntosh, 1968). They are intriguing due to their narrow host range and their marked tendency to produce persistent virus infections in vivo (MHV in mice) and in vitro (MHV in murine cell cultures, and HCV 229E in human cell cultures). This implies a highly evolved inter-relationship with the host. They cause mainly respiratory and gastrointestinal infections in man and animals. The clinical disease in man, so far as is known is mild, whereas in animals may be severe, occurring in epidemics which are of great economic importance to agriculture e.g. transmissible gastroenteritis (TGEV) in pigs, and avian infectious bronchitis (IBV) in chickens.

The number of officially recognized members of the family Coronaviridae has increased with each report of the International Committee on Taxonomy of Viruses and as of the third report stands at 11 (Table 1.) (Siddell, Anderson, Cavanaugh, Fujiwara, Klenk, MacNaughton, Pensaert, Stohlman, Sturman and van der Zeijst, 1983). The names of the viruses have been derived either in association with the disease syndrome, the host or both. Many more isolates have been reported which meet the morphologic and to some extent the molecular criteria for inclusion in the group, but are as yet insufficiently characterized and are regarded as candidate family members.

TABLE 1*

Members of the Coronavirus Family**-Grouped by Host

Designation	Name	Host	Diseases
IBV	Avian Infectious Bronchitis Virus (numerous strains)	Chicken	Tracheobronchitis
TCV	Turkey Coronavirus	Turkey	Bluecomb, Enteritis
MHV	Mouse Hepatitis Virus (numerous strains)	Mouse	Hepatitis, Enteritis, Encephalomyelitis and Vasculitis
RCV	Rat Coronavirus	Rat	Pneumonia, Rhinotracheitis Sialoacryoadenitis
TGEV	Transmissible Gastro-enteritis Virus	Pig	Gastroenteritis
HEV	Hemagglutinating Encephalomyelitis Virus	Pig	Encephalomyelitis, Gastroenteritis
PEDV	Porcine Endemic Diarrhea Virus	Pig	Enteritis
BCV	Bovine Coronavirus	Bovine	Gastroenteritis
HCV/229E	Human Coronavirus	Human	Respiratory Disease
HCV/OC43	Human Coronavirus	Human	Respiratory Disease
CCV	Canine Coronavirus	Dog	Gastroenteritis
FIPV	Feline Infectious Peritonitis Virus	Cat	Peritonitis Respiratory Disease

* Adapted from Siddell et al., 1983.

** Other candidate viruses, i.e. Human enteric coronavirus, Rabbit coronavirus, Foal enteritis coronavirus (horse) and coronaviruses from non-human primates are not included in this list.

The geographic distribution of many coronaviruses is known to extend over several continents and is considered to be worldwide. A seasonal incidence of infection occurs with HCV and TGEV. Coronaviruses predominantly infect the respiratory tract of their natural vertebrate hosts, being transmitted by the aerosol route, and these natural hosts are believed to form the reservoirs for further infection. Infection by the fecal/oral route also has been suggested, and vertical infections have been reported for IBV and MHV strains (Siddell et al., 1983; Sturman and Holmes, 1983). Although coronavirus infections are generally believed to be extremely host restricted, natural and experimental transmission to other species has been reported. Human (OC 43) and avian coronaviruses were transmitted to mice by the intracerebral (i.c.) route and there is evidence of TGEV replication in dogs, foxes and cats. Feline and canine coronaviruses were also infectious for pigs. Transmission to other hosts may lead to inapparent infections or diseases which do not occur under natural conditions (reviewed by Wege, Siddell and ter Meulen, 1982).

The pathogenesis of coronaviruses is reflected by the characteristic route of transmission: either the respiratory system in the case of HCV, IBV, MHV, TCV and MHV or the gastrointestinal tract in the case of BCV, CCV, TGEV and MHV.

Respiratory infection is confined to the ciliary epithelium of the trachea, nasal mucosa and the alveolar cells of the lungs. A local immune response resulting in secretion of IgA usually overcomes the acute phase of the disease and the development of a systemic humoral immunity hinders a severe involvement of other organs.

The enteropathogenic coronaviruses selectively infect absorptive and crypt cells of the intestinal mucosa resulting in atrophy of the villi. Virus strains vary in their predeliction for a particular site and cell type and the severity of disease varies from mild transient enteritis to a rapidly progressing fatal diarrhoea. As with respiratory infection, the local immune response provides the most important line of defense against enteric infection (Bhatt and Jacoby, 1977; Carthew and Sparrow, 1981; Hierholzer, Broderson and Murphy, 1979).

In general, as illustrated by many MHV strains which cause hepatitis or encephalomyelitis, coronaviruses cause acute lytic infections which destroy the host cell. This is considered to be the basic pathogenic mechanism involved.

In the case of HEV infection of pigs the resulting disease is characterized by vomiting and sometimes accompanied by encephalomyelitis (vomiting and wasting disease). The disease is initiated by an apparent infection of the respiratory tract, tonsils and intestines, which spreads along nerve tracts to peripheral ganglia and the central nervous system. Subsequently, the infection of neurons which regulate peristaltic functions of the intestinal tract results in the characteristic disease syndrome and, in particular, young animals may die of starvation (Andries and Pensaert, 1980a, b; Andries, Pensaert and Callebaut, 1978).

In animals, coronaviruses readily establish persistent infections which often lead to diseases of a chronic nature. Persistent infections are also readily established in cell culture (Chaloner-Larsson and Johnson-Lussenburg, 1981a, b; Lucas, Flintoff, Anderson, Percy, Coulter and Dales, 1977; Lucas, Coulter, Anderson, Dales and Flintoff, 1978; Stohlman, Sakaguchi and Weiner, 1979; Yoshikura and Tejima, 1981; Lavi,

Gilden, Highkin and Weiss, 1984; Leibowitz, Bond, Anderson and Goss, 1984). Little is known of the mechanisms governing persistent infections in vivo and in vitro, but some factors which influence the outcome of the infection in animals have been identified.

Murine coronaviruses have provided valuable in vivo models for the study of chronic and persistent disease processes in the mouse. Elucidation of the mechanisms of virus induced demyelination in these animal systems may be useful in understanding the etiology and pathogenesis of human demyelinating diseases such as multiple sclerosis (Lavi et al., 1984). It has been hypothesized that the chronic demyelination induced by MHV-JHM in mice is due to a cytolytic infection of the oligodendrocytes, the myelin producing cells (Fleury, Sheppard and Raine, 1980; Lampert, Sims and Kniazeff, 1973). In chronic MHV infections, viral nucleic acids can persist in mice for months, even though no virus or antigen can be detected. Viral sequences detected by in situ hybridization were found only in the white brain matter during chronic infection (Lavi et al., 1984), suggesting that oligodendrocytes may be the target cells for chronic infection.

Some of the major factors which determine the outcome of these processes are related to virus replication (such as virulence and tropism), whereas others are determined by the host (such as the immune response) (Wege, Koga, Watanabe, Nagashima and ter Muelen, 1983). It has been postulated that the lytic destruction of tissue by the interaction of virus with the host cells must be mitigated to allow the host to survive (Haase, Ventura, Johnson, Norrby and Gibbs, 1981). Thus the viral genetic information might be stably conserved within certain cells with expression of viral antigens being sufficienty curtailed to allow

them to escape detection and elimination by the immune system.

Knowledge about the molecular biology of the coronaviruses is relatively recent. There are reports of the growth of coronavirus (MHV) in enucleated cells (Wilhelmsen, Leibowitz, Bond and Robb, 1981) or the growth of virus in the presence or absence of actinomycin-D (Siddell, Wege and ter Meulen, 1983; Brayton, Ganges and Stohlman, 1981), which question whether a host nuclear function is required for coronavirus replication. There is also very little data regarding the early events of adsorption, penetration and uncoating involved in coronavirus replication. It is assumed for example, that upon entering the cell the positive-stranded genome directs synthesis of one or more proteins (polymerases) whose function is to transcribe the genomic and subgenomic mRNA via a replication intermediate. Assembly of virions is restricted to the cytoplasm where progeny virions are formed by a budding process from membranes of the rough endoplasmic reticulum (Massalski, Coulter-Mackie and Dales, 1981; Holmes and Behnke, 1981). The generally accepted mechanism of virus release from the cell is via fusion of virus-filled vesicles with the plasma membrane (Doughri and Storz, 1977).

Studies using molecular and immunological methods, have yielded fragmentary data with respect to relationships between different coronaviruses or within pathogenic and non-pathogenic closely related members of a species. Antigenic relationships among coronaviruses present a complex pattern and have been difficult to analyze, possibly due to the close association of the virion with cell associated material.

Structurally, coronaviruses are pleomorphic, enveloped viruses having a diameter of 80 to 220 nm. They are ether labile which indicates the presence of essential lipid in the envelope. Club shaped

peplomers are seen on the surface of the virion (Fig. 1 and 2) and are about 20 nm in length. The group derives its name from the characteristic crown-like appearance of the virion envelope (Latin corona meaning crown) when stained with phosphotungstic acid and observed in the electron microscope. This envelope appears to contain an inner and outer shell when seen in thin sections by electron microscopy. The ribonucleoprotein (RNP) has been seen as either a long strand 1 to 2 nm in diameter (Kennedy and Johnson-Lussenburg, 1975/76; Davies, Dourmashkin and MacNaughton, 1981) or as a helical single stranded RNP condensed into a coiled structure of varying diameters (Kennedy and Johnson-Lussenburg 1975/76; MacNaughton, Davies and Nermut, 1978; Caul, Ashley, Ferguson and Eggleston, 1979; Massalski, Coulter-Mackie and Dales, 1982). The virions have a density of about 1.18 gm/cm^3 as determined in equilibrium sucrose gradients. Reports of the genome size vary depending upon the particular virus, the host system used for propagation and the investigator (Table 2). Methods of preparation of the virus and RNA have also been shown to effect the final product however the RNA genome is now generally accepted to have a molecular weight around 6x10^6 daltons.

Thus, coronavirus RNA is the largest known linear single stranded animal virus RNA and is often referred to as 60S RNA to distinguish genome RNA from other subgenomic fragments. It is of positive polarity (Spaan et al., 1981) with the poly A tracts at the 3'-end (Lai and Stohlman, 1981) and functions as a messenger RNA (mRNA) in the cell (Lai and Stohlman, 1978). Genomic RNA has also been found to be infectious in appropriate cell cultures in MHV (JHM) (Wege et al., 1978) and TGEV (Brian et al., 1980). The isolated genomic RNA has been used for in

Figure 1

Electron micrograph of negatively stained (A) human coronavirus 229E and (B) the persistent VH human coronavirus.

Peplomers are clearly seen at the virion periphery. Virions were stained with phosphotungstic acid and examined in a Phillips 300 electron microscope. The bar marker represents 100 nm.

Electron micrographs courtesy of Dr. C.M. Johnson-Lussenburg.


A
B

TABLE 2

Size of Coronavirus Genomic RNA.

Virus	M.W.	Investigator
IBV	3×10^6	Tannock, 1973
	8×10^6	MacNaughton and Madge, 1977, Lomnicizi and Kennedy, 1977
	9×10^6	Watkins, Reeve and Alexander, 1975
MHV	5.4×10^6	Wege, Muller and ter Meulen, 1978
(JHM)	6.5×10^6	Wege et al., 1978
(A59)	6×10^6	Lai and Stohlman, 1978
	5.6×10^6	Spaan, Rottier, Horzinek and van der Zeijst, 1981
	6.1×10^6	Leibowitz and Weiss, 1981
HCV (229E)	5.8×10^6	MacNaughton and Madge, 1978
TGEV	6.8×10^6	Brian, Dennis and Guy, 1980

in vitro (rabbit reticulocyte extract) and *in vivo* (frog oocyte) translation studies (Leibowitz, Weiss, Paavola and Bond, 1982; Stern and Sefton, 1984). In addition, there is a methylated cap structure at the 5'-end (Lai, Patton and Stohlman, 1982a, b; Spaan, Rottier, Horzinek and van der Zeijst, 1982).

Between 5 to 9 virus-specific structural and non-structural proteins have been reported to occur during coronavirus replication. They have been identified by immunoprecipitation of ^{35}S-methionine-labelled proteins from infected cell lysates with specific antibodies followed by dissociation of the immunoprecipitates and analysis on SDS-polyacrylamide gels (Bond, Anderson and Leibowitz, 1984; Stern and Sefton, 1984). Although the situation is not entirely clear, the concensus is that all coronaviruses have three major structural proteins (Fig. 2). These are the nucleocapsid, the matrix and the peplomer proteins. The most studied and characterized components are those in the mouse (MHV) and avian (IBV) coronaviruses.

The nucleocapsid contains a non-glycosylated (N) protein with a molecular weight of 50,000 to 60,000 (50K to 60K) which is complexed with the genome as a helical ribonucleoprotein (RNP) (Siddell et al., 1983). It is phosphorylated and an associated protein kinase activity has been reported. The virus envelope contains 2 major proteins. The largest envelope protein (E2) is the surface peplomer which gives the virion its characteristic appearance when examined under the electron microscope. The E2 peplomer is a glycoprotein with a molecular weight of 180,000 (180K) which is thought to be a dimer under certain conditions which dissociates into a 90K protein (Siddell et al., 1983; Sturman and Holmes, 1983).

Figure 2

Schematic model of coronavirus structure.

Genome (RNA), nucleocapsid protein (N), matrix protein (E1), and peplomer protein (E2) shown. Taken from Sturman et al., 1980.

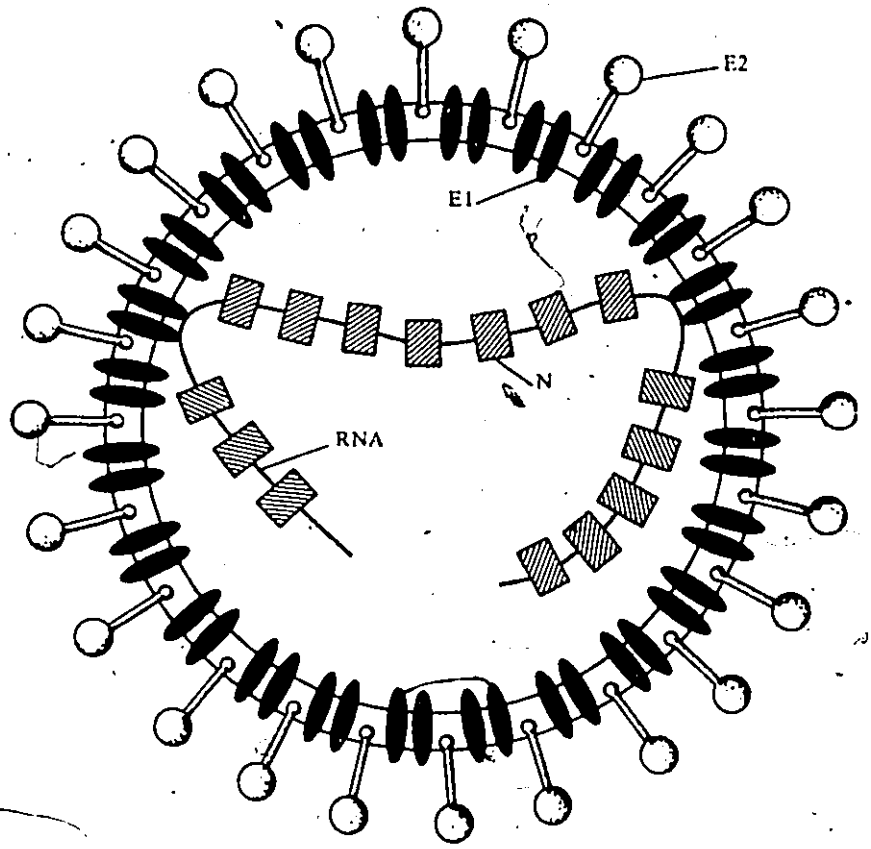
E2
E1
N
RNA

The E2 glycoprotein can be removed from the whole virion by protease treatment. It is similar to the majority of viral glycoproteins characterized so far, in that it is N-glycosylated as determined by inhibition of glycosylation of polypeptides on asparagine residues by tunicamycin (Niemann and Klenk, 1981a, b).

The E2 protein is responsible for virus attachment and cell-to-cell fusion when it occurs and elicits neutralizing antibodies during infection (Stern and Sefton, 1982). Virions (MHV) which have been released from cells treated with tunicamycin, lack the peplomer protein and are unable to attach to cells or initiate infection.

The second envelope protein (E1) is a smaller 20-35K transmembrane glycoprotein which spans the lipid membrane and is oriented so that the glycosylated region is exterior to the virion envelope (Rottier, Brandenburg, Armstrong, van der Zeijst and Warren, 1984). There has been some suggestion that the inner portion interacts with the genome (Sturman and Holmes, 1984). The E1 protein has been shown to be glycosylated by two different mechanisms, depending upon the virus family and possibly on the host cell. In tunicamycin inhibition studies, MHV E1 protein has been shown to be O-glycosylated i.e. not blocked by tunicamycin (Niemann and Klenk, 1981a, b), whereas the avian IBV E1 protein has been shown to be N-glycosylated (Niemann and Klenk, 1981a, b; Niemann, Boschek, Evans, Rosing, Tamura and Klenk, 1982; Stern and Sefton, 1982). This was the first report of 'O' glycosylation in vertebrate viruses. It appears that the E1 proteins of BCV (Niemann and Klenk, 1984) and of HCV 229E are similar to MHV (Kemp et al., 1984).

Besides these characteristic proteins, there are other proteins of various sizes which have been described, notably a 14K protein for IBV

and MHV, and glycoproteins of about 60-70K for MHV, BCV and HEV. In the case of MHV, it has been suggested that these latter may be degradation products of the large 180K dimer structure of the E2 protein or perhaps as in the case of IBV, produced by post-translational cleavage of a cell associated precursor, GP155 (Stern and Sefton, 1984).

In early studies of the swine coronaviruses, the lipids of the virion envelope of TGEV were studied (Garwes, Pocock and Wijaska, 1975). The virion envelope was shown to contain phospholipids, glycolipids, cholesterol, diglycerides, triglycerides and free fatty acids in proportions approximately corresponding to those in the cell membrane. When grown in different cell types the virion envelope reflected the lipid content of the host cell membrane (Pike and Garwes, 1977). It was concluded that the lipid bilayer of the coronavirus was derived from the host.

Antigenic studies on the coronaviruses have produced controversial results. Due to the variability and complexity of the antigens associated with coronaviruses, antigenic relationships have been difficult to assess with certainty. In many cases it is obvious that cell associated protein was causing cross reactions and difficulty in the interpretation of results. Relationships have been determined between individual members of the group and also between strains within a given species by a wide variety of tests such as immunodiffusion, complement fixation, hemagglutination, neutralization, immunofluorescence, and enzyme immunoassays. The source of antibodies for these tests was from polyvalent sera from naturally infected animals or immune sera from animals (usually rabbits) hyperimmunized with viral antigens (propagated in a variety of host systems) that had been purified to varying degrees.

Coronaviruses contain three major antigens each corresponding to the three types of virion protein; N, E1 and E2. These antigens can be differentiated using antibodies prepared against purified virion subcomponents (Collins, Knobler, Powell and Buchmeirer, 1982; Hasony and MacNaughton, 1981, 1982; Schmidt and Kenny, 1981, 1982; Yaseen and Johnson-Lussenburg, 1981). Immunological studies by immune electron microscopy with monoclonal antibodies or with antisera against subcomponents prepared from purified virions, indicate that the antigenic sites responsible for the induction of neutralizing antibodies are associated with the surface peplomer polypeptides (Snyder and Marquardt, 1984; Koolen, Osterhaus, Siebelink, Horzinek and van der Zeijst, 1984).

Immunological studies now indicate that the coronaviruses can be divided into avian and mammalian groups. Both the avian coronaviruses and the mammalian coronaviruses can be further subdivided into two antigenic groups (Table 3) (Gerna, Cereda, Revello, Cattaneo, Battaglia and Torsellinni-Gerna, 1981; Horzinek, Lutz and Pedersen, 1982; MacNaughton, 1981; MacNaughton, Madge and Reed, 1981; Maru and Sato, 1982; Pedersen, Ward and Mengeling, 1978; Pensaert, De Bouck and Reynolds, 1981; Reynolds, Garwes and Lucey, 1980; Schmidt and Kenny, 1981).

As more knowledge of the structural components has become available, it has been possible to better understand their relationship to replication events.

TABLE 3

Antigenic Relationships of Coronaviruses and Classification into Groups.

	Group 1	Group 2
Mammalian	HCV 229E (several serotypes)	HCV OC43 (several serotypes)
	TGEV (1 serotype)	MHV (many serotypes)
	CCV (1 serotype)	RCV (SDAV) (1 serotype)
	FIPV (1 serotype)	BCV (1 serotype)
		HEV (1 serotype)
Avian	IBV (at least 8 serotypes)*	TCV (1 serotype)

* The number of serotypes for all strains may increase as further studies evolve.

The mechanism of coronavirus replication is now reasonably clear. Most coronaviruses replicate *in vitro* within 12 hours at 37oC. Infection is often accompanied by cytopathic changes, either syncytium formation or vacuolation followed by cell disintegration. There are very little data on the early events, such as adsorption, penetration and uncoating, associated with coronavirus infection. In the case of HCV 229E, virions initially attach over the whole cell surface and are then re-distributed away from the cell periphery by an energy requiring process (Patterson and MacNaughton, 1981). MHV3 uptake is rapid and temperature dependent (Krzystyniak and Dupuy, 1981). Uptake was not related to the phagocytic capacity of the cells and might involve a mechanism such as receptor-mediated endocytosis (Helenius, Fries, Garoff and Simons, 1980). The location and mechanism by which the nucleocapsids are uncoated after entering the cell is unknown.

Early studies with Actinomycin-D (Act-D) were conducted to determine whether the virus could replicate without the host cell DNA function. The cells were treated at the time of, and at various times after infection, with Act-D. It was found that MHV, IBV and RCV grew equally well in the presence or absence of Act-D (Malluci 1965; Lomnicizi and Kennedy, 1977; Parker, Cross and Rowe, 1970). Furthermore, virion-associated polymerase could not be detected, providing additional support for the positive polarity of the coronaviruses.

In the case of HCV 229E, partial inhibition of replication by Act-D was found (Kennedy and Johnson-Lussenburg, 1979). It was reported that the target for Act-D inhibition was maximally sensitive within the first 10 hours of replication and it was postulated that a short-lived host product was involved in virus replication. This putative product was suggested to be associated with virus maturation since normal levels of viral RNA production occurred, but markedly reduced levels of infectious virus.

In other experiments, when cells were pre-treated with Act-D for 1 hour prior to infection and infection synchronised by adsorbing virus at 0-4°C, a small but reproducible synthesis of RNA could be demonstrated (Brayton, Lai, Patton and Stohlman, 1982; Cheley, Anderson, Cupples, Lee, Chan and Morris, 1981a; Cheley, Morris, Cupples, and Anderson, 1981b). This synthesis was suggested to represent production of negative strand RNA by polymerase which is believed to have been translated from incoming genomic RNA. This 'early' RNA polmerase (in the case of MHV) was detected within 1 hour post infection. A second or 'late' RNA polymerase activity was found at 6 hours post infection. The early RNA transcripts were reported to be mainly negative-stranded whereas the

products of the late polymerase were primarily positive-stranded (Brayton et al., 1982). It was suggested that the negative strand RNA would serve as template for the production of the positive-stranded RNA and a replicative intermediate was postulated. Such a replicative intermediate (RI) consisting of a single species which corresponds to the full length MHV genomic RNA has been reported (Lai et al., 1982b; Lai, Baric, Brayton and Stohlman, 1984).

During coronavirus infection, six 3'-co-terminal subgenomic RNAs which form a nested set extending in the 5' direction are produced. These are synthesized in non-equimolar amounts but in relatively constant proportions (Stern and Kennedy, 1980a, b; Spaan et al., 1981; Wege, Siddell, Sturn and ter Meulen, 1981a, b; Leibowitz, Wilhelmsen and Bond, 1981). The molecular weights of these subgenomic RNAs range from the smallest 0.6×10^6 to the largest 6×10^6 which is similar to genome size. This largest genome sized RNA is termed RNA 1 and the smaller RNAs are numbered accordingly (Fig. 3). The subgenomic RNAs so far reported are all capped and polyadenylated. All subgenomic and a portion of the genome-sized RNA molecules are associated with polysomes throughout infection (Spaan et al., 1981; Wege et al., 1981a). The messenger function of the MHV positive-stranded RNA species has been demonstrated in vitro (Cheley et al., 1981a; Rottier, Spaan, Horzinek, and van der Zeijst, 1981; Siddell, Wege, Barthel and ter Meulen, 1981).

The genome RNA of IBV and its 5 subgenomic mRNA species have been compared using T_1-RNase resistant oligonucleotide finger printing (Stern and Kennedy, 1980a, b). Together, the 5 subgenomic species greatly exceeded the total size of the genomic RNA, suggesting that the subgenomic RNAs shared some sequences. Comparison of T_1 oligonucleotide di-

Figure 3

Nested-set structure and expression of the murine hepatitis virus genome.

The largest RNA is termed RNA 1 and smaller RNAs are numbered accordingly. They form a 3'-co-terminal nested-set extending towards the 5'-end of the genome. All the RNAs are polyadenylated at the 3'-end, are positive-stranded and have messenger function. RNA 1 is structurally identical to genome RNA. Each gene is identified as the unique coding region (A-G) on the 5'-end of each RNA. The coded proteins have been tentatively designated after *in vitro* translation. The size of the translation product for each mRNA corresponds approximately to the coding potential of the 5'-sequences which are absent from the next smallest mRNA. From Siddell et al., 1983.

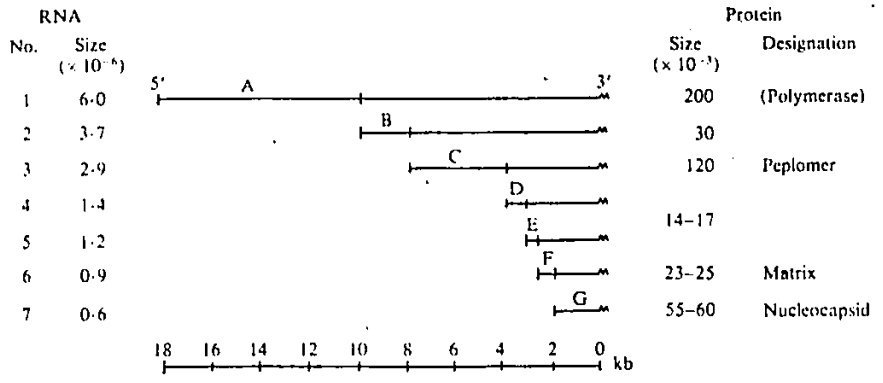
RNA
No.
Size
(× 10⁻⁶)
Protein
Size
(× 10⁻³)
Designation
5'
3'
A
B
C
D
E
F
G
1
6·0
200
(Polymerase)
2
3·7
30
3
2·9
120
Peplomer
4
1·4
5
1·2
14–17
6
0·9
23–25
Matrix
7
0·6
55–60
Nucleocapsid
18
16
14
12
10
8
6
4
2
0
kb

gests of these intracellular RNAs revealed that they formed a nested set of sequences. The oligonucleotides of each mRNA species were contained within the next larger mRNA species, starting from the 3'-end. This also showed that the genomic RNA was of the same positive sense as the mRNA since they shared the same oligonucleotides.

By ordering the T_1 oligonucleotides of the genomic RNA through analyses of poly(A)-containing fragments, they showed that all of the subgenomic mRNAs shared common sequences extending from the 3'-terminus of the genome.

Similar data were reported for MHV (Spaan et al., 1981; Wege et al., 1981b; Weiss and Leibowitz, 1981; Cheley et al., 1981a; Lai et al., 1981). The relative molarity of each mRNA was estimated by densitometry of electrophoresis gels. They concluded that the molar weight increments from the smallest to the largest mRNA, probably represented 5'-terminal extension and that because the sum of the molar weights of the six subgenomic mRNAs exceeded the genome size, the mRNA sequences probably overlapped.

No structural difference between the genome RNA and the genome-sized intracellular mRNA has been described (Brayton et al., 1982; Cheley et al., 1981a; Lai et al., 1981, 1982a; Leibowitz et al., 1982; Mahy, Siddell, Wege, and ter Meulen, 1983; Spaan et al., 1981, 1982; Wege et al., 1981b; Weiss and Leibowitz, 1981).

The 5'-ends of all MHV A59 mRNAs shared a common sequence (5'-cap-N-UAAG). Each mRNA contained a T_1-oligonucleotide which was designated as No. 10. Interestingly, oligonucletide No. 10 was not found in the same position within each mRNA species examined. This oligonucleotide was found only once in the oligonucleotide fingerprints of the virion

genomic RNA (Lai et al., 1982a, 1984; Spaan et al., 1982). From these data, it was suggested that oligonucleotide No. 10 represented a leader RNA segment which was joined to the body sequences of every mRNA. Since this oligonucleotide had 23 bases, and the first 5 nucleotides at the 5'-ends of mRNAs were found to be identical for all of the mRNAs (Lai et al., 1982a), it was suggested that the leader sequence had to be at least 28 nucleotides long. The unique nucleotides which were found only in the mRNAs were thought to represent the junction oligonucleotides between the leader and the body sequences of mRNAs. This was consistent with the base sequences of these oligonucleotides, which showed that they were identical at the 5'-half, but differed at the 3'-half. The 5'-half sequences were presumably derived from the leader and the 3'-half sequences were presumably derived from the body sequences of the mRNAs.

The replication of MHV was not impaired in cells treated with Act-D (Mahy et al., 1983) indicating that cellular RNA synthesis was not required. The synthesis of each mRNA was inactivated by UV irradiation in proportion to its own length (Jacobs, Spaan, Horzinek and van der Zeijst, 1981). Thus the subgenomic mRNAs were not derived from the cleavage of precursor RNAs. Furthermore, the nascent RNA chains in the RI structure contain the leader sequences, suggesting that the leader sequences were not added to the mRNA post-transcriptionally, but were probably synthesized independently and then served as primer for the synthesis of mRNAs. This indicated that the leader RNA and the body sequences of MHV RNAs had to be joined by a novel nucleus-independent mechanism. The most likely model proposed that the leader RNA was synthesized independently and fell off the negative-stranded RNA tem-

plate. This free leader RNA then was then bound to RNA polymerase or to a short complementary region at the initiation sites for different mRNAs. In this fashion the leader RNA served as a primer for mRNA synthesis (Lai et al., 1984).

The mRNA function of several of the MHV subgenomic viral RNAs has been demonstrated in vitro, and the mRNAs encoding each of the virion proteins, or its precursors, have been identified (Stern and Sefton, 1984). In MHV infected cells, the synthesis of each viral polypeptide was initiated independently (Cheley and Anderson, 1981; Siddell et al., 1983). RNA 7, the smallest RNA, encoded N, the intracellular nucleocapsid polypeptide (60K). The unique region of the next smallest, RNA 6, coded for the matrix protein polypeptide (23K) in vitro, or its glycosylated counterpart (25K) in Xenopus laevis oocytes. The third major intracellular RNA, RNA 3, coded for the peplomer protein core (120K), the in vitro translation product, or the co-translationally glycosylated peplomer precursor (150K) in oocytes (Cheley et al., 1981b; Leibowitz et al., 1982; Rottier et al., 1981; Siddell et al., 1983). The translation products of two further MHV RNAs, RNA 2 and RNA 4/5, have been identified as corresponding to 30K and 14-17K intracellular viral polypeptides respectively (Liebowitz et al., 1982; Siddell et al., 1983). MHV genome sized RNA has been translated in vitro to produce a group of polypeptides of greater than 200K (Leibowitz et al., 1982) which are suggested to be components of the virus-specific RNA polymerase found in infected cells.

After synthesis, genomic RNA and virion proteins were assembled in the cytoplasm at the rough endoplasmic reticulum and virions budded into the cisternae, acquiring their lipid membranes from the cell. The

virions were subsequently transported through, and accumulated in, the Golgi complex and smooth-walled vesicles. Sites for the insertion of E1 and E2 glycoproteins were presumably different, as indicated by the tunicamycin studies, however they have not been precisely located. There was an absence of budding from the plasmalemma. The mechanism of virus release has not been characterized (Beesley and Hitchcock, 1982; Ducatelle, Coussement, Pensaert, Debouck and Hoorens, 1981; Holmes, Doller and Sturman, 1981; Massalski et al., 1981, 1982; Siddell et al., 1983; Sturman and Holmes, 1983).

Nucleic acid homology has been used to investigate the relationships between strains by comparing the genomes of several coronaviruses. The two main techniques used have been nucleic acid hybridization and nucleic acid fingerprinting. Most of the investigations have been between various MHV strains with a few studies reported on the human strains HCV 229E and OC 43 or avian IBV strains. The data reported so far have given an incomplete picture of the molecular relationships between coronaviruses.

Molecular hybridization using cDNA prepared from mRNA 7, representing the MHV A59 nucleocapsid, revealed 70-80% homology between four MHV strains. This probe represented only 5% of the genome and the nucleocapsid gene is the most likely to be conserved among MHV strains (Cheley et al., 1981a, b). In other studies, using cDNA representative of the entire MHV genome (termed cDNA rep.) or cDNA representative of only the 3'-end of the genome (termed cDNA-3') sequence homologies of 74%-90% were reported among weakly pathogenic A59, hepatotropic MHV-3 and neurotropic JHM strains (Weiss and Leibowitz, 1983).

The degree of homology was partially reflected in T_1-resistant oligonucleotide fingerprints of MHV genomes (Lai and Stohlman, 1981). This technique examines only about 10% of the sequences i.e. only those large enough to form spots by 2-dimensional gel electrophoresis, and is considered by some to be too sensitive to small changes, even single base changes in large nucleotides, and thus may overemphasize small differences in sequence (Weiss and Leibowitz, 1983). Using this technique, more extensive divergence in MHV strains maintained under persistent conditions as compared to MHV strains maintained under lytic conditions was demonstrated (Lai et al., 1983).

However, studies on the avian coronaviruses using T_1 RNase-resistant oligonucleotide fingerprinting, tended to illustrate the oversensitivity of this technique. The genome RNAs of 13 isolates of IBV were examined and although identified as IBV isolates by other criteria, produced 11 quite distinct fingerprints. Different serotypes gave different fingerprints as might be expected, but so did varieties within a serotype. This raised the question of which virus isolate should in fact be considered the prototype strain (Clewley, Morser, Avery and Lomniczi, 1981).

Both techniques are valuable tools for the investigation of molecular relationships at the genome level. Hybridization serves to reveal major differences when probes are used representing most or all of the sequences of the virus genome, whereas oligonucleotide fingerprinting serves to identify such differences.

RATIONALE FOR RESEARCH

The investigation of the biology of the human coronavirus infection has been hampered because HCVs are notoriously fastidious, their host range being usually restricted to the natural host. *In vivo* and *in vitro* persistent infections of mouse cells by Mouse Hepatitis Virus (MHV) are well established and serve as a model system for the study of demyelinating disease (Herndon, Griffin, McCormick and Weiner, 1975; Lucas et al., 1977; Stohlman and Weiner, 1978; Leibowitz et al., 1984).

In order to understand the mechanisms of persistence, the molecular biology of coronaviruses has been intensively studied. Most studies have focussed on MHV or JHM coronaviruses of the murine system (Lucas et al., 1977; Stohlman and Weiner, 1978; Hirano et al., 1981; Holmes and Behnke, 1981; Lavi et al., 1984; Leibowitz et al., 1984). In 1978, an *in vitro* persistent infection with the human coronavirus HCV 229E was established in L132 cells, a human embryonic lung cell line (Chaloner-Larsson and Johnson-Lussenburg, 1981a).

Preliminary biological study of these viruses revealed that the persistent state might be associated with the class of non-cytocidal infections transmitted through cell division (Chaloner-Larsson and Johnson-Lussenburg, 1981a, 1981b). This implies that all the cells contain copies of the viral genome and that expression of the genome requires host permissiveness. Acute or persistent infections of the same cell type were dependent on the temperature of incubation.

Phenotypic differences between the parental 229E and persistent VH viruses, were characteristic of these infections. The VH virus was more cytocidal in L132 cells at 33°C than 229E virus. The VH virus also demonstrated a greater efficiency of replication at the optimal temperature of 33°C as it consistently produced higher titres of infectious virus, and a faster growth curve. Antigenically the 229E and the VH viruses seemed to be identical. Virus shedding from the persistently infected cells was temperature dependent, in that at 37°C, the optimal temperature for the cells, the cells continued to grow and continuously produced high titres of infectious VH virus, whereas at 33°C cell death occurred resulting in a characteristic lytic infection.

The persistently infected cells were characterized and found to be resistant to super-infection with the homologous 229E virus but permitted replication of poliovirus, a different group. No reverse transcriptase activity was detected indicating that a retrovirus or other source of reverse transcriptase was not present in the system and ruled out incorporation of the genome as a possible mechanism of persistence. No evidence of DI particles was found, again ruling out a second possible mechanism of persistence.

Recently, the presence of small amounts of interferon (IFN) was detected by neutralization with antibodies to HuIFN- and HuIFN-B, suggesting that in addition to temperature, IFN was involved in the mechanism of persistence.

The VH virus has remained phenotypically stable through hundreds of passages of the persistently infected cell line, and the persistently infected cell line could be frozen and recovered after extended periods of time.

In order to further elucidate the changes in the virus progeny resulting from the persistent infection, it was of interest to undertake a comparative study of the RNA genomes of the parental 229E and persistent VH human coronaviruses. The purpose of this investigation was to:

1. Isolate and characterize 229E and VH RNA.
2. Synthesize cDNA probes for each RNA.
3. Compare genome RNAs by liquid and solid phase hybridization.

II. MATERIALS AND METHODS

Suppliers of products, reagents and equipment are listed in Appendix I.

1. VIRUS

The human coronavirus 229E (HCV 229E) was originally isolated in secondary human kidney tissue culture (Hamre and Prochnow, 1966). The source of the present seed virus was the Laboratory Centre for Disease Control (LCDC) in Ottawa which had received the original seed virus in September, 1969 from Dr. R. Chanock, N.I.H., Bethesda, Maryland. The virus had been passaged twice in Human Embryonic Skin fibroblast cell cultures at LCDC and was tested and found to be free of mycoplasma.

2. CELLS AND CELL CULTURE

(a) Media

All cells were grown in Eagles Minimal-Essential Medium (MEM) with Earles balanced salts. The MEM was supplemented with 10% fetal calf serum (FCS), 200 mM glutamine, 2.0 g/L of $NaHCO_3$, 100 units/mL of penicillin, 100 ug/mL of streptomycin and 50 ug/mL of neomycin. When kanamycin was used it was at a concentration of 100 ug/mL.

For plaque tests, an overlay medium composed of Medium M199 containing 0.2% $NaHCO_3$, 2% FCS, antibiotics and 0.6% of Oxoid Agar No. 1. containing 50 ug/mL 5-bromodeoxyuridine (BUDR), and 200 ug/mL diethylamino-ethyl dextran (DEAE-dextran). The BUDR was included to enhance the plaque counts and to produce larger clearer plaques and the DEAE-dextran to maintain the quality of the monolayer (Hamre, Kindig and Mann, 1967, Bradburne and Tyrrell, 1969).

(b) L132 Cells

The continuous human embryonic cell line L132 (Davis and Brolin, 1960) was obtained from the cell bank at LCDC. It had originally been received from the American Type Culture Collection in 1970. It was stored in liquid nitrogen and recovered as required to start new stocks. It was tested for the presence of mycoplasma (Barile and Kern, 1971) at our passage levels 6, 10, 12, 14, 18 and 21 and found negative. The cells were used between passages 5 and 50 for production of virus and plaque assays.

Confluent monolayers in 75 cm^2 flasks were trypsinized twice per week. They were split at a ratio of 1:3 or 1:4 as required. The planting concentration was approximately 100,000 cells/mL. Each flask received 30 mL of cell suspension (3 million cells/flask or 40,000 cells per cm^2). Confluent monolayers were obtained in approximately 3 days at 37°C. A yield of approximately 10 million cells/flask was regularly found by viable cell counts using trypan blue.

(c) Persistently Infected (HV-1) Cells

The persistently infected HV-1 cell line was originally established in 1978 (Chaloner-Larsson and Johnson-Lussenburg, 1981a, 1981b). The successful maintenance of these persistently infected cells was directly related to the temperature of incubation subsequent to initial infection with 229E virus. Persistently infected cells were maintained by regular passage (3 times/week) and incubation at 37°C.

These cultures were a stable population of cells which appeared normal and grew at rates characteristic of L132 cell cultures and continuously shed virus into the medium at titres of 10^5 to 10^6 pfu/mL per 48 hours. Persistently infected cells were stored in liquid nitrogen

and revived without difficulty whenever a new stock was required. These cells were tested for the presence of mycoplasma at various passage levels and found to be positive. Various methods were attempted to eliminate the mycoplasma species present, however none were successful.

3. VIRUS PROPAGATION

HCV 229E and persistent VH virus (virus derived from persistently infected HV-1 cells) were propagated as acute infections in L132 cells. Cell monolayers were inoculated at an approximate multiplicity of infection of 1.0, adsorbed for 1 hour at ambient temperature, fed with serum-free MEM and incubated at 33°C for 40 hours. Virus was stored at -70°C either as whole infected cultures or as supernatant fluid (SNF) which had been clarified at 1000xg at 4°C for 20 minutes. Persistent VH virus shed from the persistently infected cells was also harvested 48 hours after passaging of HV-1 cell cultures. Supernatant fluids containing the persistent VH virus were collected, clarified at 1000xg, and stored at -70°C for further concentration.

To prepare radioisotope labelled virus, the cells were infected as described above, but at the end of the adsorption period, 10 uCi/mL of 5-^{3}H uridine (specific activity 25 Ci/mmol) was added to the MEM. In some experiments 1 ug/mL of actinomycin-D (Act-D) was included in the MEM (i.e. added post adsorption).

4. PLAQUE ASSAY

Virus was titrated by plaque assay in monolayers of L132 cells in 75 cm^{2} flasks (Kennedy and Johnson-Lussenburg, 1975/76). Aliquots of 0.33 mL of virus dilutions were inoculated on to each monolayer and allowed to adsorb for 1 hour at ambient temperature with re-distribution

of the inoculum every 20 minutes. At the end of the adsorption period, the monolayers were overlaid with 30 mL/flask of plaque overlay medium which had been previously equilibrated at 45°C. The agar was allowed to solidify at ambient temperature and the flasks were incubated upside down at 33°C for 6 days. At the end of the incubation period, each culture was covered with 10 mL of 5% formol-saline in order to inactivate infectious virus and to fix the cells. After 1 hour at ambient temperature the agar and formol-saline was removed. Finally, the cells were stained with 1% crystal violet and the plaques counted.

5. VIRUS PURIFICATION AND CONCENTRATION

Two methods were used for the purification and concentration of viruses.

(a) The Density Gradient Method

HCV 229E or VH infected radiolabelled cultures were first subjected to three freeze-thaw cycles to release virus and produce a cell lysate suspension. The lysate was clarified at 1000xg for 20 minutes at 4°C. The supernatant was removed and the cellular debris was discarded. Radiolabelled virus was harvested from the supernatant by pelleting onto a 65% w/v sucrose cushion at 48,000xg at 4°C for 60 minutes in Beckman SW28 rotor. The 4 mL of interface material was collected via a peristaltic pump. The interface material was pooled. This was placed in an ultrafiltration cell at 4°C with an XM 300 membrane and washed free of sucrose using 1 mM phosphate buffer at pH 7.2. The resulting virus concentrate, now in phosphate buffer, was further purified by rate zonal (velocity) centrifugation through a preformed 10-35% w/w sucrose gradient at 63,000xg at 4°C for 90 minutes in a Beckman SW28 rotor. Gra-

dients were fractionated into 2 mL aliquots from the bottom of the centrifuge tubes. A 50 uL sample of each fraction was read on a refractometer to determine the sucrose concentration. From each fraction 100 uL was added to 10 mL of scintillation cocktail and counted in a Beckman LS 250 scintillation counter. The peak fraction containing radioactive virus, plus one fraction on either side of the peak were pooled, washed and concentrated by Amicon ultrafiltration as before (Kennedy and Johnson-Lussenburg, 1975/76).

The virus concentrates were then layered onto preformed linear 25-65% w/w sucrose gradients in 1 mM phosphate buffer pH 7.2, and centrifuged to equilibrium at 63,000xg at 4°C for 18 to 24 hours in a Beckman SW41 rotor. 500 uL fractions were collected from the bottom of each tube. A 10 uL sample per fraction was read on a refractometer. Another 10 uL sample per fraction was added to 3 mL of scintillation cocktail and counted. The peak fractions were pooled and pelleted at 97,000xg for 120 minutes in a Beckman FA 50 rotor. The pellets were resuspended in 100 uL of 1 mM phosphate buffer and used immediately or stored at -70°C (Chaloner-Larsson and Johnson-Lussenburg, 1981).

(b) The Polyethylene Glycol Precipitation Method

At 40 hours post infection, SNF's were removed from infected cultures and clarified at 1000xg at 4°C for 10 minutes. The clarified SNF's were first adjusted to 2.2% NaCl (0.4M) and then to 10% polyethylene glycol 6000 (PEG) using stock solutions of 22% NaCl and 30% PEG. Virus was precipitated at 4°C for 18 hours and pelleted at 10,000xg at 4°C for 30 minutes (Wege et al., 1978). Infected cell monolayers were covered with 5 mL of 1 mM phosphate buffer pH 7.0 and frozen.

6. PREPARATION OF RNA

A variety of extraction procedures exist for the isolation and purification of RNA. The utility of each depends to a large extent on the nature and source of the starting material. Some methods use phenol (Perry et al., 1972), SDS (Hiatt, 1962), or proteinase K and detergents (Glisin et al., 1974).

The RNA genome of the various coronaviruses is usually considered to be fragile. In order to obtain as large a part of the genome as intact as possible two approaches were used to obtain RNA. Two sources of virus were used: virus obtained after sucrose density gradient purification or virus obtained after PEG precipitation. The main concern with any extraction procedure was to prevent possible contamination of preparations with RNases. RNases are extremely hardy and rapidly digest any RNA isolated. Therefore, in an attempt to preclude RNase activity the following precautions were observed.

All procedures were performed wearing disposable gloves in a work area restricted to work with RNA and the use of disposable latex gloves. All procedures were performed in an ice bath. All solutions, where possible, were treated with diethylpyrocarbonate (DEP) for at least 1 hour and autoclaved. The DEP combines with protein and when autoclaved destroys the protein and therefore any RNases (Fedorcsak and Ehrenberg, 1966). Glassware was immersed in a nitric acid or chromic acid bath overnight. It was thoroughly washed in double distilled water and siliconized with dichlorosilane. All glassware was baked overnight at 250°C. Disposable microcentrifuge tubes and micropipettor tips were autoclaved.

For the extraction of RNA, virus pellets were resuspended individually in 1 mL of TES buffer (10 mM tris-HCl pH7.2, 1 mM EDTA, 100 mM NaCl), adjusted to 0.5% SDS detergent (Na dodecylsulfate), 200 ug/mL of proteinase K was added and, after thorough mixing was incubated with shaking at 37°C for 30 minutes. A phenol-chloroform extraction was then performed by adding equal volumes of a 1:1 mixture of re-distilled phenol and chloroform saturated with TES. These mixtures also contained 8-hydroxy quinoline (0.1%) which acts as an anti-oxidant, as a partial inhibitor of RNase and as weak chelator of metal ions (Kirby, 1956). The mixtures were thoroughly mixed and centrifuged in a microfuge at 12,800 rpm/10 minutes (10,000xg). The aqueous phases were carefully removed and pooled in siliconized, baked 30 mL Corex tubes and adjusted to 0.2M ammonium acetate (NH_4Ac). Two volumes of cold ethanol were added and the RNA was allowed to precipitate at -20°C for 18 hours. The RNA precipitate was centrifuged at 10,000xg at 4°C for 30 minutes. The supernatant was removed and the RNA pellet was dried under vacuum. The dried RNA was dissolved in 100 uL of DEP treated water (DEP water) and samples were withdrawn for A_{260} readings or for scintillation counting. For long term storage the RNA was stored either under ethanol or as a dried preparation at - 70°C.

7. ELECTROPHORESIS

Electrophoresis was conducted by standard methods (McMaster and Carmichael, 1977). Samples for electrophoresis were denatured by adding a mixture of 1.0 M glyoxal and 50% dimethylsulfoxide (DMSO) in 10 mM phosphate buffer pH 6.8 to the RNA and heating at 50°C for 60 minutes. The glyoxal and the DMSO were routinely de-ionized immediately prior to use with a mixed bed resin until the pH was neutral. Gels consisted of

1.5% agarose cast in a horizontal apparatus. Gels were run submerged under 10 mM phosphate buffer pH 6.8 and the buffer was constantly recirculated between the reservoirs to maintain the neutral pH required for the stability of the glyoxal-guanosine adducts. The samples were electrophoresed at a constant 100 volts for 120 minutes.

Prior to loading each sample, sterile loading buffer consisting of 50% glycerol, 10 mM phosphate buffer pH 6.8 and 0.4% bromphenol blue was added to each sample to monitor migration. RNA size markers were routinely included in each gel. These were 16S and 23S E. coli RNA and 4S yeast RNA. However, a suitable size marker for the expected 60S viral genomic RNA was required. Glyoxal-denatured RNAs and DNAs fall on the same log molecular weight versus relative mobility curve which makes it possible to estimate RNA molecular weights using easy to obtain DNA fragments of known size as markers (McMaster and Carmichael, 1977). Therefore, a preparation of lambda DNA digested with the restriction enzyme Hind III, was used to provide markers (Szybalski and Szybalski, 1979). Hind III digestion of lambda DNA generates 8 fragments (23.5, 9.7, 6.6, 4.3, 2.2, 2.1, 0.47 and 0.13 kb). The 23.5 kb fragment migrates approximately equivalent to the 60S viral genomic RNA.

After electrophoresis, the glyoxalation of RNA was reversed by soaking the gel in 50 mM NaOH for 1 hour. The gel was washed 3 times in 50 mM phosphate buffer at pH 6.8 and stained with ethidium bromide. It was washed again and photographed under UV light, using a Polaroid MP3 camera.

In order to detect the ^{3}H-labelled RNA present in the gels, the gels were dehydrated with three 10 minute washes in ethanol. This was followed by soaking in a 3% solution of 2,5-diphenyloxazole (PPO) in

ethanol for 18 hours. The gel was then washed in water to precipitate the PPO. The gel was placed in a slab gel dryer, covered with a piece of Whatman filter paper and Saran Wrap and dried under vacuum for 1 hour. Heat (60°C) was applied only for the last half hour of drying to avoid cracking of the gel. The dried gel was placed on a sheet of Kodak XAR film in a Kodak cassette with intensifying screens and fluorographed at -70°C for varying lengths of time (Bonner and Laskey, 1974).

DNA preparations were run under exactly the same conditions and treated in the same manner. The gels were stained with ethidium bromide and photographed under UV light to locate the DNA molecular weight marker bands.

For autoradiography of cDNA labelled with ^{32}P, the wet gel was wrapped in Saran Wrap, placed on a sheet of Kodak XAR film in a Kodak cassette and autoradiographed at ambient temperature for varying lengths of time.

8. SELECTION OF POLYADENYLATED (POLY [A+]) RNA

Purified RNA was heated in TE buffer (10 mM Tris-HCl pH 7.4 and 10 mM EDTA) at 80° to 90°C for 2 minutes. It was then quickly cooled on ice, and NaCl was added to 0.5 M. This solution was then passed over an oligo-deoxythymidylic acid (oligo-dT cellulose) column equilibrated in binding buffer (0.5 M NaCl, 10 mM Tris-HCl pH 7.4, 1 mM EDTA, 0.2% SDS). The unbound material was removed by washing the column with three or more volumes of binding buffer. Polyadenylated acid (poly A+) RNA was released from the column by eluting in TE buffer with 0.1% SDS. The RNA in the eluate was ethanol precipitated as previously described (Maniatis, Fritsch and Sambrook, 1980).

9. INFECTIVITY OF mRNA

Positive-stranded RNA is supposed to be infectious. In order to evaluate the 229E RNA for infectiousness, the salt shock method was selected to introduce the RNA into the susceptible host cells (Wecker, Hummeler and Goetz, 1962). Poly (A+) or mRNA was initially treated with 1.4 M $MgSO_4$ while monolayers of L132 cells were pre-incubated with saline containing 0.02 M $MgSO_4$ for 15 minutes at 37°C. The conditioned cells were then overlaid with pre-treated virus RNA mixed with DEAE-dextran (0.5 mg/mL). After 25 minutes adsorption at ambient temperature, the cells were washed with saline and MEM containing 2% FCS. A series of blind passages was carried out in order to try to amplify the virus. The monolayers were overlaid with plaque media as usual and monitored for plaque development at 33°C (Wege et al., 1978).

10. PROBE SYNTHESIS

Complementary DNA (cDNA) probes were synthesized using avian myeloblastosis (AMV) reverse transcriptase. Genome RNA from purified virus, which is known to be of positive polarity, was used as template. The cDNAs were labelled with [5'-d ^{32}P]-thymidine triphosphate to a specific activity of 3.4×10^7 cpm/ug. To synthesize cDNA representative of the entire coronavirus genome ($cDNA_{rep.}$), a procedure using oligomers of calf thymus DNA as random primers was used (Weiss and Leibowitz, 1981, 1983; Valotaire, Tenniswood, LeGuellec and Tata, 1984). Oligo-dT_{12-18} primer was used for synthesis of short cDNA representating the 3' end of the RNA genome (cDNA-3'). The cDNAs were synthesized in the presence 100 ug/mL of Act-D to ensure the synthesis of mainly single stranded cDNA which was required for liquid hybridizaton experiments.

11. LIQUID HYBRIDIZATION

Liquid hybridization reactions were conducted as described by Britten et al., 1974. Incubations were carried out at 68°C in 0.3 M NaCl at various nucleic acid concentrations and times. A minimum of 100-fold excess driver sequences were always used in relation to tracer component. Each time point had at least 1000-2000 cpm of tracer. Reaction mixtures were prepared in hybridization buffer and 4 uL was loaded into siliconized capillary tubes, flame sealed and stored frozen. At the time of use, capillary tubes were boiled for 3 minutes and placed at 68°C to hybridize. At appropriate time intervals, capillaries were placed into a dry ice/ethanol bath. Upon completion of the whole hybridization reaction, capillaries were broken open and emptied into 200 uL S_1 nuclease buffer (50 mM Na acetate, 100 mM NaCl, 1 mM ZnCl and 10 ug/mL denatured calf thymus DNA). Each sample was split into two portions. One served as a control and the other was digested with 20 units of S_1 nuclease. Digestion proceeded at 42°C for 45 minutes.

To each sample was added 200 uL of 50% tri-chloro acetic acid (TCA) and 600 uL of carrier RNA (tRNA 150 mg/mL) and placed on ice for 30 minutes to allow the RNA to precipitate. Each sample was filtered under vacuum in a Millipore Manifold fitted with Whatman GF/C filter discs. Each reaction tube was washed 3 times with cold 5% TCA to ensure removal of all traces of the digest and the washings were added to the appropriate filter. Each filter was then washed 3 times in cold ethanol, placed in open scintillation vials and placed into a 37°C oven until dry. Three mL of scintillation cocktail was added to each filter and the radioactivity was counted in a scintillation counter. All samples were tested in duplicate.

Percent hybridization was calculated using the following formula:

$$\frac{\text{(cpm in nuclease treated sample - background)}}{\text{(cpm in nuclease untreated sample - background)}} \times 100$$

The background count represents the zero time or "snap back" hybridization radioactivity and is subtracted from each value.

Kinetic analysis of nucleic acid association by base pairing is a valuable technique for determining the complexity and relatedness of sets of nucleotide sequences (Appendix II). In the case of RNA-DNA reassociation reactions, the value is expressed as a R_0t value. The R_0t values were calculated as being the product of the RNA concentration and the time of incubation (expressed as moles of ribonucleotides/litres/sec). The 50% R_0t value represents the value that is needed to allow hybridization to proceed halfway to completion.

12. NORTHERN BLOT HYBRIDIZATION

HCV 229E, VH and L132 cellular RNAs were glyoxalated to denature the RNA, electrophoresed in agarose gels and blotted onto membrane supports (Thomas, 1980; Meinkoth and Wahl, 1984). The solid supports used were PALL biodyne nylon membranes which are claimed to be 500 fold more efficient than nitrocellulose in RNA transfers using the method of Thomas (1980). This sensitivity is comparable to that obtained with diazo-benzyloxymethyl paper in that picogram (pg) quantities of nucleotides can be detected with higher resolution and lower backgrounds. The protocol supplied with the biodyne membranes was followed closely in order to optimize the hybridization procedure. The bound RNA was then hybridized with cDNA to each individual template RNA and autoradio-

graphed (Alwine, Kemp and Stark, 1977).

In order to reduce background reactions, several experiments were performed in which northern blots were treated with pre-hybridization reaction mixtures which included non-labelled cDNA prepared to cellular RNA template and/or calf thymus random primer.

III. RESULTS

1. PURIFICATION AND CONCENTRATION OF VIRUS

A standard preparation of HCV 229E seed virus was prepared and stored at -70°C. Thereafter, when a new batch of virus was produced and titrated in the plaque assay, the seed virus was included as a control in order to assess any variability in test results. Titres ranged from 1.6×10^7 to 3.9×10^7 pfu/mL over a period of 2 years. The ingredients in the plaque overlay media were compared from 2 laboratories and were identical except for the Noble Agar No. 1 (Oxoid). Batches of this agar had to be pre-tested to ensure good production of plaques. Only those allowing production of large plaques were accepted for use in plaque assays.

Virus concentration and purification using sucrose gradient and molecular sieving procedures (Fig. 4) was slow, labor intensive, limited by equipment, expensive and provided small yields. It also required many manipulations during which virus degradation and loss of infectivity took take place making it difficult to estimate concentration factors.

Peaks were readily identified in the gradients when the virus was labelled with ^{3}H-uridine. The density of the virus in the peaks was determined in equilibrium sucrose gradients. The virus band was found in the 43% sucrose fraction which corresponds to a density of 1.18 g/cm^3. Material from virus peaks was centrifuged at 97,000xg for 2 hours, the pellet resuspended in 100 uL of 1 uM phosphate buffer (pH 7) and stored frozen at -20°C until the viral RNA was extracted.

Figure 4

Flow Chart of Purification 229E and VH Viral RNA

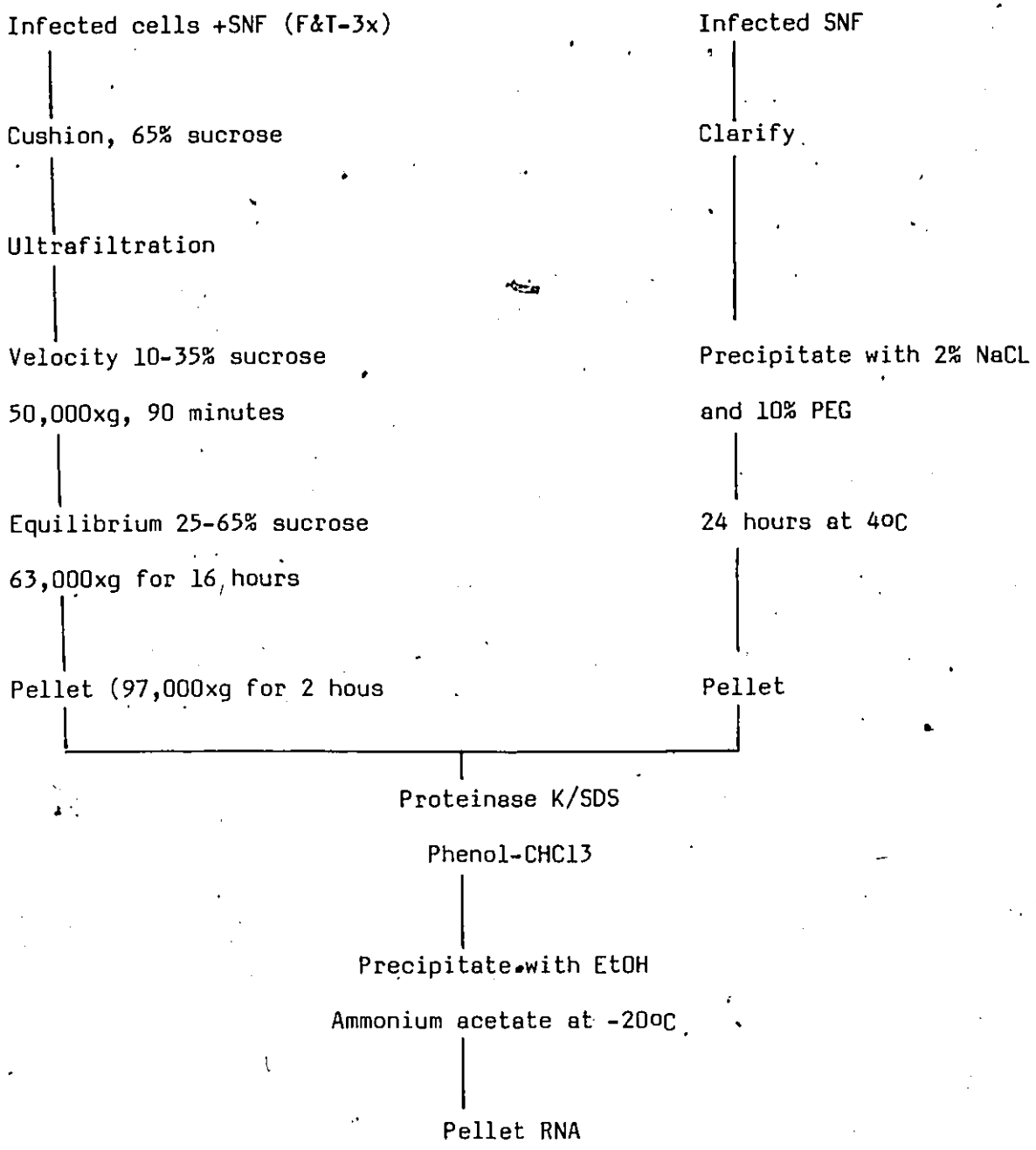

The second protocol employing PEG 6000 and NaCl was used to reduce the number of manipulations and exposure of the virus to nucleases. The advantages were immediately apparent as larger batches (2000 mL versus 200 mL) of virus could be processed in 24 hours as compared to 5 days by the first method. Concentration factors were readily determined after concentration as infectivity of the virus was maintained. Typical concentration factors were from 25 to 60 times based on titres of original virus. This procedure did not produce a preparation as purified as the gradient method but was adopted due to its rapidity and the necessity to circumvent problems arising from the presence of RNases. Leading authors in this area have found and recommended that best results are obtained by methods which are rapid and direct in order to reduce the possibility of RNase contamination and digestion, which can occur even when stored at very low temperatures with a variety of RNase inhibitors (Lai and Stohlman, 1978; Weiss and Leibowitz, 1983).

Initially, RNA was extracted using 1% SDS and heating at 37°C, from virus purified by the first protocol. Sucrose gradients of such material seldom produced a sharp peak of 60S RNA (Fig. 5). Usually RNA containing fractions comprised a large portion of the gradient indicating that various sizes of RNA were present and that degradation of the RNA had probably occurred. A further complication was that, initially, when HCV 229E was propogated, it was not labelled with isotope in the presence of Act-D as Act-D had been shown to curtail production of infectious virus (Kennedy and Johnson-Lussenburg, 1975/76). As a result cellular RNA as well as viral RNA was probably labelled.

Figure 5

Velocity sucrose gradient of RNA extracted from 229E by SDS and heat

Purified 229E virus was treated with 1.0% SDS and heated at 37°C. The resultant product was loaded onto a 5-25% sucrose gradient and centrifuged at 35,000 rpm for 4.5 hours. Fractions were collected and radioactivity counted.

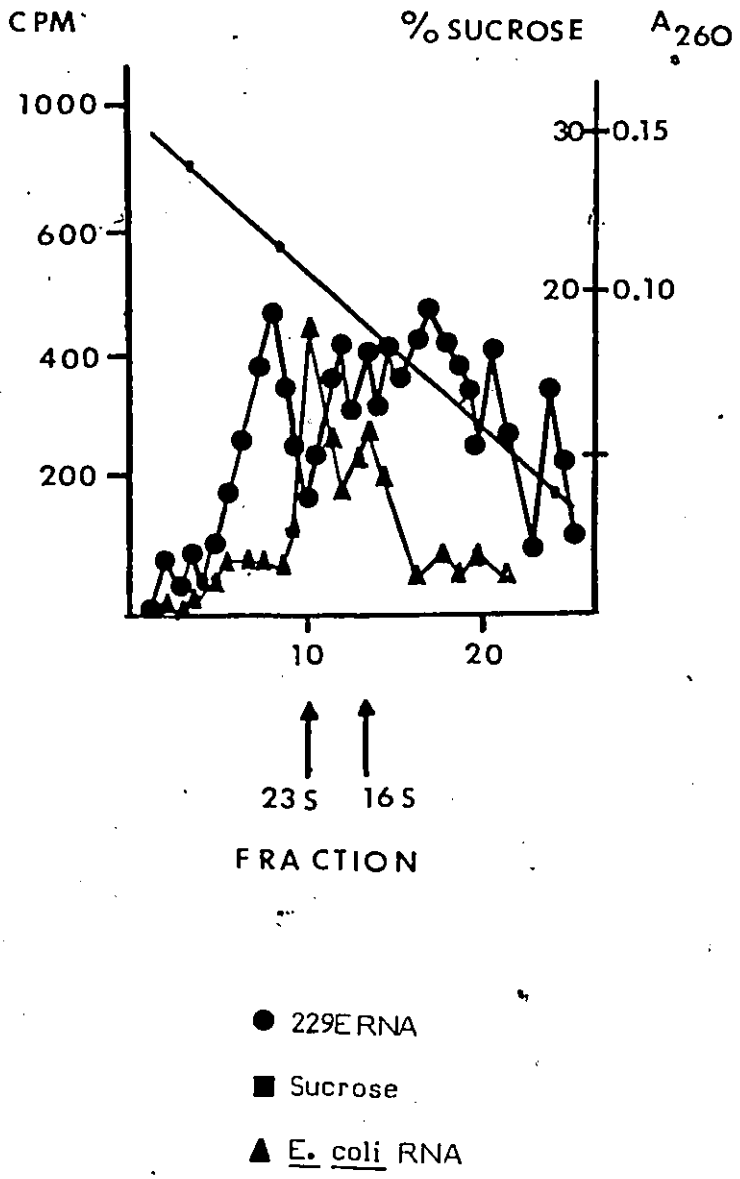
CPM
% SUCROSE
A_{260}
1000
600
400
200
30
20
0.15
0.10
10
20
23 S
16 S
FRACTION
229E RNA
Sucrose
E. coli RNA

Using the second method of RNA extraction (Maniatis, 1980) with PEG purified virus, clean peaks on gradients were achieved (Figure 6). The use of SDS and digestion with proteinase K followed by extraction with phenol and chloroform reduced residual protein, however, when excess protein was suspected phenol/chloroform extraction was repeated several times until A_{260}/A_{280} values of 2.0 were obtained for the alcohol precipitated extract indicating that the RNA was essentially free of any protein. RNA was then precipitated with 2 volumes of ethanol (EtOH) at - 20°C overnight, pelleted, dried under vacuum and reconstituted when required. Average yields of RNA were 8.8 ug per T75 flask for 229E virus and 17 ug per T75 flask for VH virus prepared under acute infection conditions. An average of 10^9 pfu's per flask were obtained wth 229E, and an average of 10^{10} pfu's per flask for VH virus. With these values it was possible to calculate the pfu to particle ratio for each virus.

$$\frac{\text{Average mw nucleotide (320)} \times \text{Nucleotides (20,000)}}{\text{Avogadro's number } (6.023 \times 10^{23})}$$

$$\text{equals RNA per virion} = 1.0 \times 10^{-11} \text{ ug/virion}$$

If the RNA from 1 virion weighs 1×10^{-11} ug, then 8.8 ug of 229E RNA represents 8.8×10^{11} virions, and 17 ug of VH RNA represents 1.7×10^{12} virions. Therefore the particle to infectivity (pfu) ratio must be 880:1 for 229E virus and 170:1 for VH virus. This may be a reflection of the fact that the VH virus was found in previous studies to be more cytocidal, to have a higher efficiency of replication and to yield higher titres.

Figure 6

Velocity Sucrose Gradient of 229E Virus RNA

Purified 229E virus was treated with SDS and proteinase K followed by phenol-chloroform extraction. The RNA was precipitated with ethanol and loaded onto a 5-25% velocity sucrose gradient which was centrifuged at 24,000 rpm for 16 hours. Fractions were collected and radioactivity counted. E. coli RNA size markers were detected by UV spectrophotometry at 260 nm.

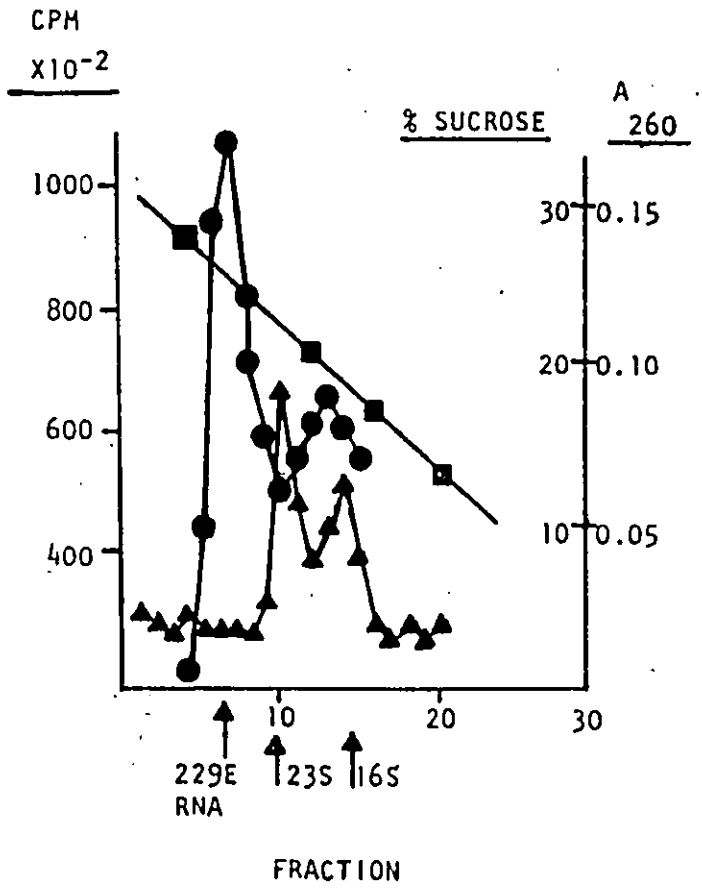
CPM
X10-2
% SUCROSE
A
260
1000
800
600
400
30
20
10
0.15
0.10
0.05
10
20
30
229E
RNA
23S
16S
FRACTION
229E RNA
Sucrose
E. coli RNA

Initially problems were encountered with visualization of the glyoxalated RNA in 1.5% agarose gels. This was due to the low efficiency of ethidium bromide intercalation with RNA under these conditions which resulted in very faintly stained smears as appearing under UV light. This procedure was modified, by treating the glyoxal-guanosine adducts with 50 mM NaOH which resulted in their complete dissociation (McMaster and Carmichael, 1977). The glyoxal then no longer interfered with ethidium bromide intercalation and stained RNA was readily seen under UV light.

In these preliminary experiments no RNA in the 60S size region could be detected but long smears of RNA were observed (Fig. 7, lanes 6 and 9). This indicated a wide range of RNA molecules were present in the gel, presumably breakdown products of the genome. RNA prepared from persistent VH virus from the supernatant fluid (SNF) of infected cultures maintained at 37°C, gave a very different result. As the cells were in good condition, and because there was no freezing and thawing to release cellular RNA and RNases, a pure viral preparation was obtained with minimum delay. When extracted by the phenol-chloroform (P-C) method and electrophoresed, the first evidence of an isolated 60S band of HCV RNA was obtained (Fig. 7, lanes 2 and 3). This result was repeatable with similarly produced batches of RNA from VH virus SNFs (Fig. 7, lanes 8, 9 and 10).

At this point a batch of 229E virus was prepared and purified by PEG precipitation directly from the SNF without freezing and thawing. The RNA was extracted by the phenol-chloroform method. After glyoxal treatment the RNA was electrophoresed on an agarose gel and a faint band in the 60S region was obtained. Further similar preparations verified

Figure 7

Agarose gel electrophoresis of 229E and VH RNAs

Viral RNA treated with glyoxal (5 ug/lane) was electrophoresed in a horizontal 1.5% agarose gel in 10 mM phosphate buffer (pH 6.8), at 100 mA for 2 hours. Bands were stained with ethidium bromide and photographed under UV light.

229E RNA lanes 4, 5, 7, 11.

VH RNA lanes 2, 3, 6, 8, 9, 10.

RNA size markers in lane 1 and 12 consisted of lambda DNA digested with Hind III restriction enzyme; the largest fragment approximates 60S size RNA.

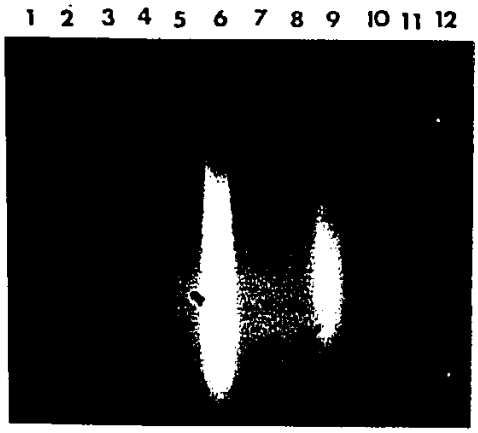
1 2 3 4 5 6 7 8 9 10 11 12
-23.5 Kb (60S)

this result. There was still one problem. In all gels long tailing smears of smaller RNA species were seen which when fluorographed were found to be radioactive.

In order to solve this problem, it was decided to re-evaluate the use of Act-D to produce virus since others, working with MHV, always used Act-D for preparation of their viral RNA (Lai and Stohlman, 1978).

An experiment was designed to determine virus production in the presence of 1 ug/mL of Act-D and the results are shown in Fig. 8. In the first 20 hours post-infection, very little difference was seen between the amount of infectious virus shed into the medium from cultures treated or not treated with Act-D. Both groups had titres in the SNF of about $3x10^6$ pfu/mL at 20 hours post-infection. By 40 hours post-infection however, a difference was observed: $4x10^6$ pfu/mL in the SNF of treated cultures, and $16x10^6$ in the SNF of untreated cultures, a 4 fold difference. No further attempts were made to determine whether titres of cell associated virus were different.

This method was adopted, even though less virus appeared to be produced in the SNF, in order to ensure that only viral RNA was labelled with isotope. The viral RNA produced by this procedure was extracted, treated with glyoxal and electrophoresed. Only a clear band in the 60S region was seen under UV light when the gel was stained with ethidium bromide (Fig. 9, lane 3). When the gel was dehydrated in alcohol, treated with PPO and fluorographed at -70°C, bands in the 60S region were observed. Only a small amount of RNA of a smaller size was evident (Fig. 14 lanes 1, 4, 7). This procedure was adopted for 229E RNA production.

When RNA from th 229E and VH viruses was electrophoresed in the

Figure 8

Comparison of 229E Virus Yields in the Presence of Actinomycin-D

Virus was grown in L132 cells either in the absence of or in the presence of 1 ug/mL of Actinomycin-D. Samples of SNF were taken at various times post infection and infectious virus was assayed by plaque test in L132 cells.

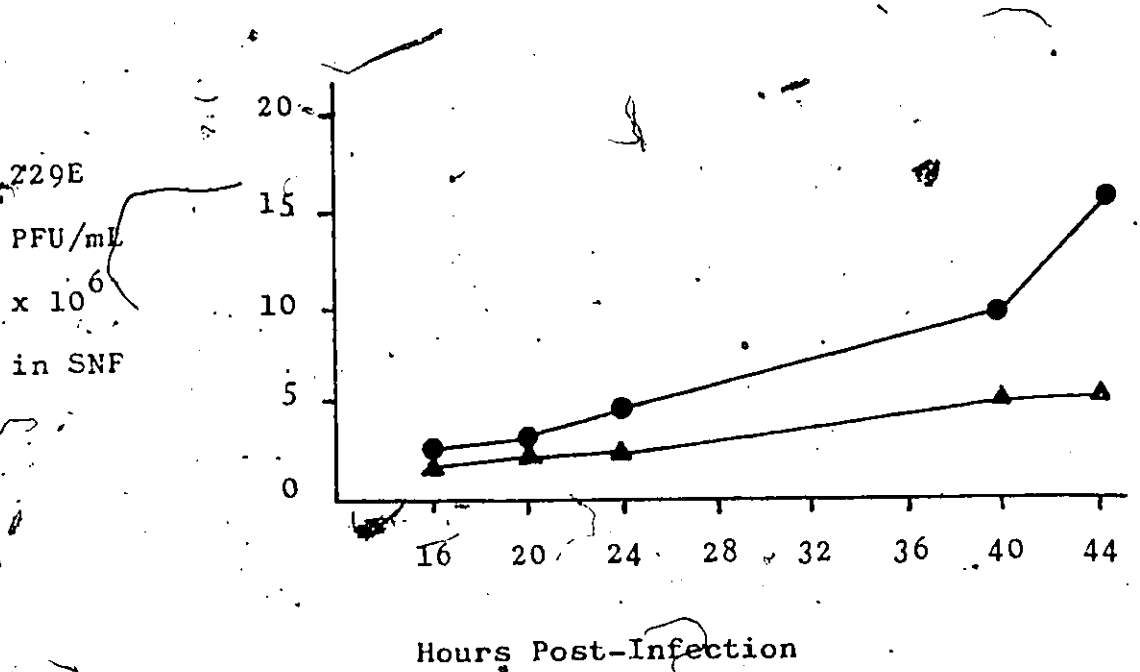
229E
PFU/mL
x 10^6
in SNF
20
15
10
5
0
16
20
24
28
32
36
40
44
Hours Post-Infection
● No Actinomycin-D
▲ Actinomycin-D 1 ug/mL

Figure 9

Agarose gel electrophoresis of 229E RNA, cellular RNA and VH RNA

Lane 1 229E RNA

Lane 2 Cellular RNA

Lane 3 VH RNA

Glyoxalated RNA was electrophoresed under acidic (pH 6.8) conditions for 2 hours at 100 V, treated with 50 mM NaOH, stained with ethidium bromide, and photographed. 229E RNA migrated 12 mm from the origin, whereas the VH RNA migrated only 10 mm from the origin. This indicates that the VH RNA is larger than the 229E RNA.

= 605

same gel under identical conditions, it was clear that the RNA of the VH virus was located nearer the origin than was the RNA of the 229E virus (Fig. 9). This result was regularly obtained with many different batches of RNA and indicated that the VH RNA was larger than the parental 229E RNA.

2. PREPARATION OF POLY (A+) RNA

Poly (A+) RNA was selected using oligo-deoxythymidine column chromatography. Poly (A+) RNA was bound under high salt concentrations and eluted under low salt concentrations (Fig. 10). The yields were very low. From 340 ug of VH RNA, separated by sucrose gradient and chromatographed on an oligo dT column, only 30 ug of poly A(+) RNA was recovered, a yield of 8.8%. An attempt to demonstrate the infectivity of this RNA was undertaken using cell shock with high salt concentration (Wege et al., 1978). The results were very marginal, as only 1 plaque was obtained. Due to the very limited quantities of RNA available this approach to further characterize the isolated product was not continued.

3. PREPARATION OF TEMPLATE RNA

The coronaviruses are known to contain positive-stranded genome RNA. Therefore the RNA extracted from purified virus was suitable for use as template for cDNA synthesis. Each preparation of RNA to be used as template was checked on agarose gels to ensure that the 60S band of genomic RNA was present.

4. SYNTHESIS OF CDNA

The synthesis of cDNA probes was initially as described by Weiss and Leibowitz, 1981. This procedure was subsequently replaced by that of Valotaire et al., 1984. The synthesis of cDNA representative of the

Figure 10

Selection of poly (A+) RNA by oligo dT column chromatography.

229E RNA was chromatographed through an oligo-dT column with binding buffer under high salt conditons (1 M NaCl). The column was washed with binding buffer and then the poly (A+) RNA was eluted under low salt conditions (Tris-HCl only). Fractions were collected and examined by UV spectrophotometry to detect peaks containing RNA.

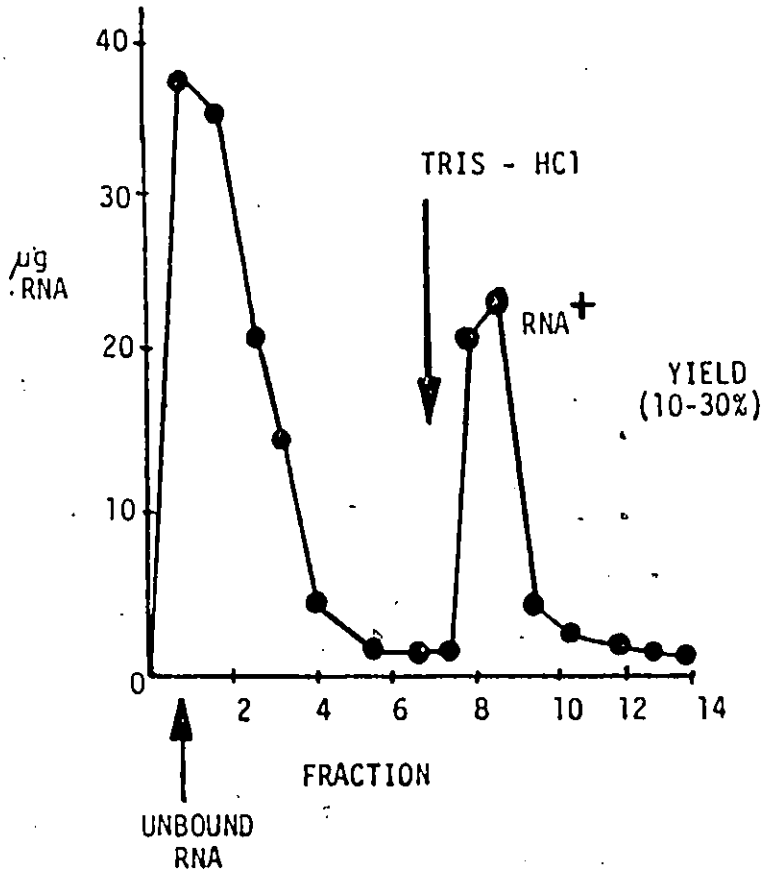
40
30
20
10
0
µg RNA
TRIS - HCl
RNA+
YIELD (10-30%)
2
4
6
8
10
12
14
FRACTION
UNBOUND RNA

whole genome was primed with calf thymus DNA random primers. The synthesis of cDNA representative of the 3'-end of the genome was primed with oligo-dT_{12-18} primer. Alpha-^{32}P-dCTP was incorporated as tracer. To assure the synthesis of single-stranded cDNA, Act-D was incorporated into the reaction mixtures (Weiss and Leibowitz, 1983). After the RNA template was hydrolyzed the size of the cDNA was determined by electrophoresis on agarose gels (Fig. 11). The relative size of the cDNAs ranged from 200 to 4000 nucleotides as estimated from molecular weight markers included in each gel. This size range was judged to be suitable for use in liquid and northern hybridization experiments.

5. HYBRIDIZATION

Liquid hybridization reactions were performed using cDNA (rep.) synthesized with 229E RNA or VH RNA as template and hybridized to 229E RNA, VH RNA and cellular RNA. As seen in the upper curve in Figure 12, the homologous reaction was very rapid, exceeding 50% at a log $R_o t$ value of 4. The heterologous VH RNA, the middle curve in Figure 12, reacts to 50% at a log $R_o t$ value of 2.2. The lower curve in Figure 12 represents cellular RNA and reached 50% at a log $R_o t$ value of 1.6.

When the hybridization mixtures were allowed to hybridize to completion in the presence of excess RNA driver, saturated plateau levels were obtained as seen in Table 4. When the values were normalized to 100% for the homologous 229E RNA/cDNA (rep.) system, there was 67% hybridization by VH RNA, the heterologous system, with the same probe. This represents a genome difference of 33%.

When VH cDNA (rep.) was used and the homologous VH RNA/cDNA (rep.) was normalized to 100%, a smaller difference of only 14% was observed with the heterologous 229E RNA.

Figure 11

Autoradiograph of agarose gel of 229E cDNA (rep.) and VH cDNA (rep.)

Lane 1 229E cDNA (rep.) glyoxal treated

Lane 2 VH cDNA (rep.) glyoxal treated

The size of the cDNA was estimated to be from 200 to 4000 nucleotides.

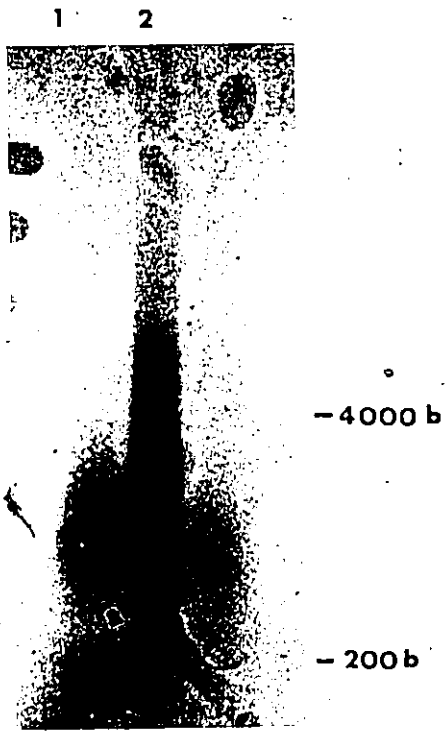
1
2
4000 b
200 b

Figure 12

Liquid Hybridization curves of 229E cDNA (rep.) hybridized with 229E RNA, VH RNA and cellular RNA.

2000 cpm of ^{32}P-cDNA (rep.) per point were hybridized to completion with varying concentrations (0.001 or 0.1 mg/mL) of 229E, VH and cellular RNA. At various times, samples were removed and hybridization was assayed by S_1 nuclease digestion. RNA concentration (R) x time (t) curves were established.

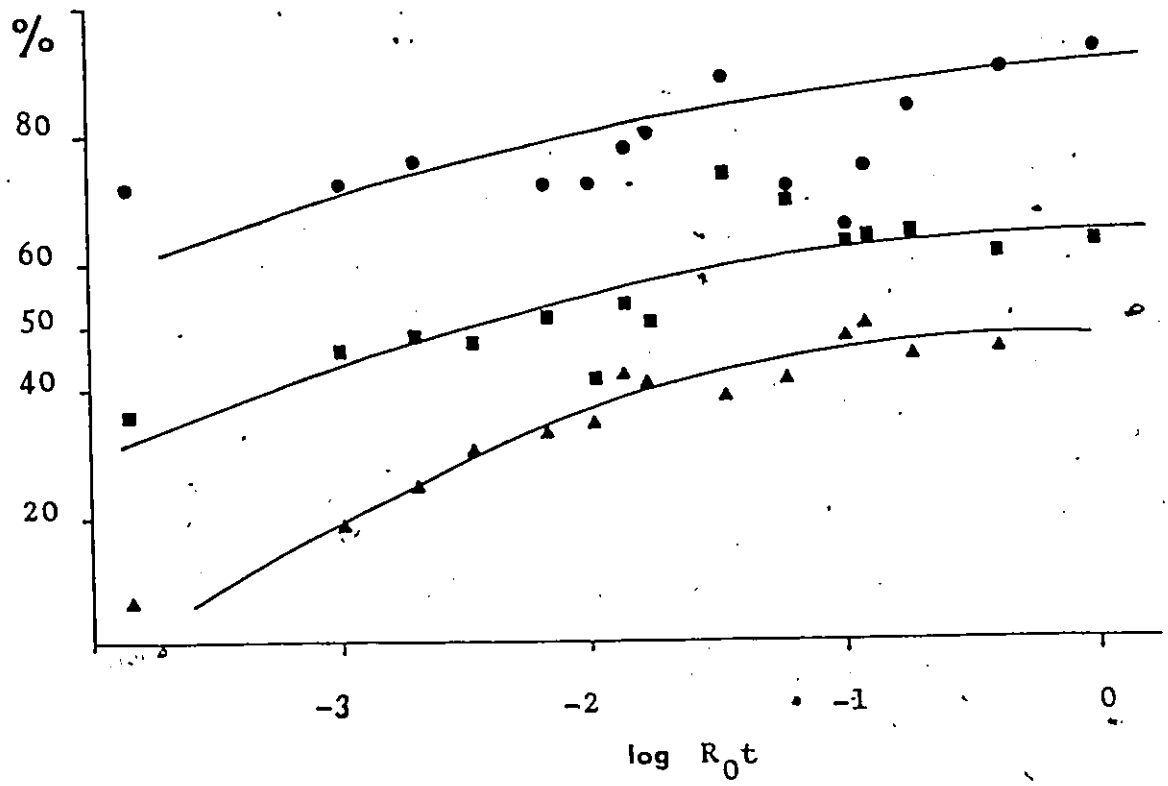

● 229E RNA

■ VH RNA

▲ Cell RNA

In both systems, a background reaction of 45% and 50% respectively was found with cellular RNA.

TABLE 4

Normalized Liquid Hybridization Values

Source of RNA	Percent Hybridization*	
	229E cDNA* (rep.)	VH cDNA* (rep.)
229E	100 (95)	86 (80)
VH	67 (64)	100 (93)
Cellular	47 (45)	60 (50)

* 229E cDNA (rep.) and VH cDNA (rep.) were cross hybridized to completion with an excess of RNA from purified virions or cellular RNA. These values have been normalized to 100% hybridization of the homologous reactions. The actual percent hybridization values obtained appear in brackets.

Northern blot hybridizations were performed using cDNA (rep.) prepared against template from 229E RNA, VH RNA and cellular RNA. The glyoxal treated RNA samples were electrophoresed in sets of 3 lanes in agarose gels. One set was removed from the gel, stained with ethidium bromide and photographed to verify the size, location and approximate quantity of each RNA before blotting onto PALL biodyne membranes (Fig. 13). A duplicate set was treated in an identical manner after blotting was complete in order to record the relative amounts of each RNA transferred (Fig. 14), and also fluorographed (Fig. 15), to assess the degree of RNA transfer. Smaller RNA species blotted more readily than larger species. Transfer of 60S RNA was evidenced by a marked decrease

Figure 13

Agarose gel of 229E RNA, VH RNA and cellular RNA prior to blotting onto PALL biodyne membranes for use in northern blot hybridization

Lane 1 229E RNA glyoxal treated

Lane 2 Cell RNA glyoxal treated

Lane 3 VH RNA glyoxal treated

RNA samples were treated with glyoxal and electrophoresed in a 1.5% agarose gel for 2 hours at 100 mA. The gel was stained with ethidium bromide and photographed by UV transillumination. The size, location and quantity of each RNA was thus verified prior to transferring onto PALL biodyne membranes used for northern blot hybridization. Size standards were electrophoresed in parallel in the positions shown.


1
2
3
-60S

Figure 14

Agarose gel of 229E RNA, cellular RNA and VH RNA post-northern blot

Lanes 1, 4, 7	229E RNA; glyoxal treated
Lanes 3, 6, 9	VH RNA; glyoxal treated
Lanes 2, 5, 8	Cellular RNA; RNA; glyoxal treated

This is the same gel as seen in Figure 13, which was used for a northern blot and then stained by ethidium bromide and photographed by UV transillumination. The reduction in staining indicates that most of the smaller and some of the 60S sized RNA was blotted to the Biodyne membrane in 24 hours. Blotting time was extended to attempt to blot more 60S RNA.

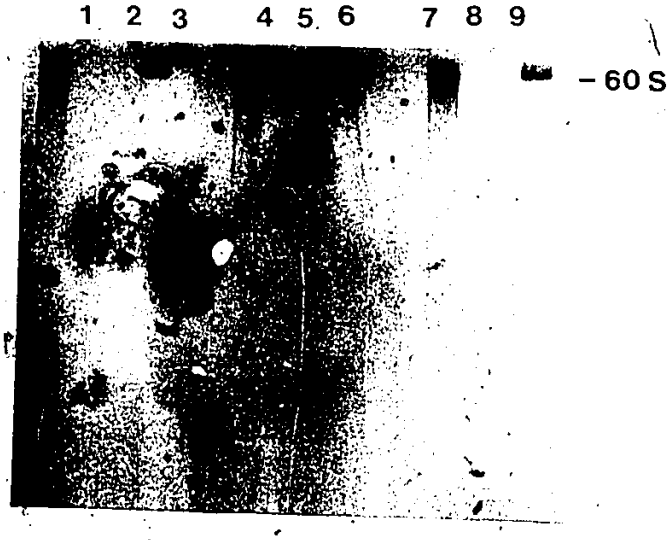
1 2 3 4 5 6 7 8 9
- 60 S

Figure 15

Fluorograph of 229E RNA, cellular RNA and VH RNA post-northern blot

Lanes 1, 5, 9	229E RNA.
Lanes 3, 6, 9	VH RNA
Lanes 2, 5, 8	Cellular RNA

Each lane originally contained equal cpm of ^{3}H-RNA.

The gel in Figure 14 was fluorographed for 9 days at -70°C.

The VH RNA appears to have transferred better than the 229E RNA as evidenced by the decrease in signal intensity in lanes 8, 12, and 16.

NOT SUITABLE FOR MICROFILMING

NE SE PRÊTE PAS AU MICROFILMAGE

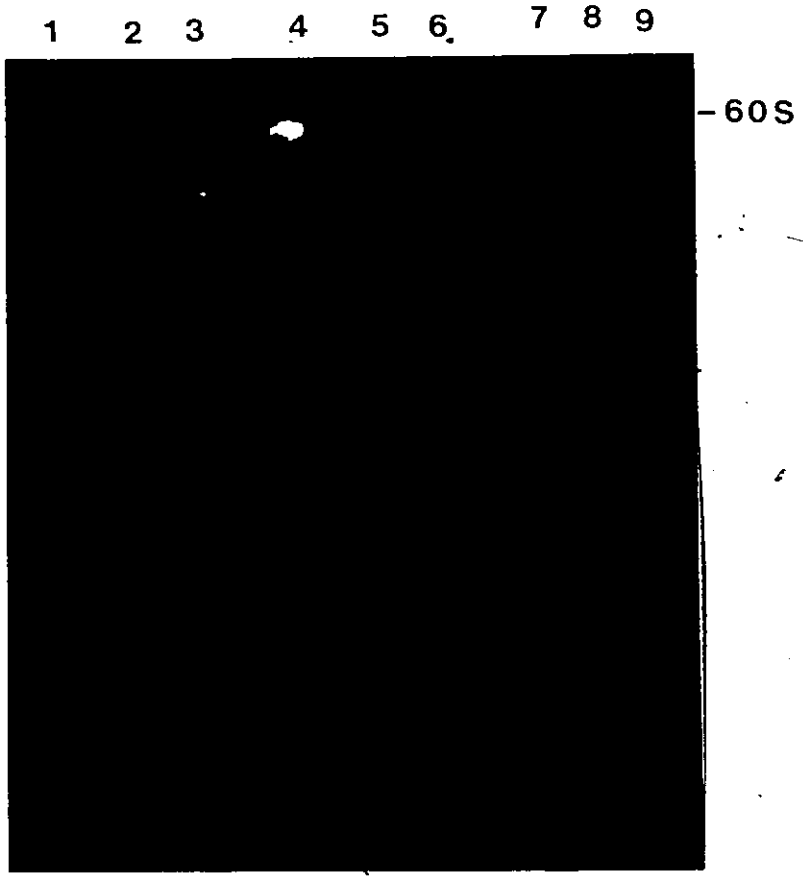

in stain intensity of this band in the gels. Blots were then autoradiographed. To reduce hybridization of cellular RNA, blots were performed using calf thymus random primers in the pre-hybridization buffer. This would serve to saturate any binding sites available from primer which was still associated with the cDNA. This gave overall reduced hybridization as well as a lower reaction with cellular RNA (Fig. 16A, B, C). 229E cDNA (rep.) hybridized strongly with 229E RNA in the 60S region only and not with the VH RNA in the 60S region (Fig. 16A). cDNA (rep.) to VH RNA hybridized strongly with VH RNA in the 60S region only and not with the 229E RNA in the 60S region (Fig. 16B). cDNA (rep.) to cellular RNA reacted strongly with cellular RNA and to a lesser degree with 229E and VH RNA (Fig. 16C).

In order to obtain more specific hybridization, cDNA was synthesized using oligo-dT_{12-18} as primer and templates from 229E RNA, VH RNA and cellular RNA. To evaluate RNA transfer, a series of blots was done with gels which had been blotted once (post-blot gels) then treated with NaOH to hydrolyze any large RNA species which may not have been blotted from the gels in the first blotting procedure.

Blots reacted with cDNA (3') prepared with oligo-dT_{12-18} primer gave clearer results but of reduced intensity, than did blots reacted with cDNA (rep.). cDNA (3') prepared to 229E RNA gave clear hybridization reactions and the distinction between the homologous and heterologous RNA was marked (Fig. 17A). cDNA (3') prepared to cellular RNA reacted very specifically with cellular RNA and very weakly to the viral RNAs (Fig. 17B). cDNA (3') prepared to VH RNA gave a very weak homologous reaction and appeared to react weakly with the cellular RNA (Fig. 17C). When RNAs were hydrolyzed post-blot and re-blotted, bands were

Figure 16

A Autoradiograph of northern blot.

Hybridization with 229E cDNA (rep.) probe

Lane 1 229E RNA

Lane 2 Cell RNA

Lane 3 VH RNA

In order to reduce hybridization with cellular RNA, the blots were pre-hybridized with calf thymus random primers.

Lanes 1, 2, 3 hybridized with 229E cDNA (rep.) probe.

B. Autoradiograph of northern blot.

Hybridization with VH cDNA (rep.) probe

Lane 1 229E RNA

Lane 2 Cell RNA

Lane 3 VH RNA

In order to reduce hybridization with cellular RNA, the blots were pre-hybridized with calf thymus random primers.

Lanes 1, 2, 3 hybridized with VH cDNA (rep.) probe.

C. Autoradiograph of northern blot.

Hybridization with cDNA (rep.) probe to cell RNA

Lane 1 229E RNA

Lane 2 Cellular RNA

Lane 3 VH RNA

In order to reduce hybridization with cellular RNA, the blots were pre-hybridized with calf thymus random primers.

Lanes 1, 2, 3 hybridized with cDNA (rep.) probe to cellular RNA.

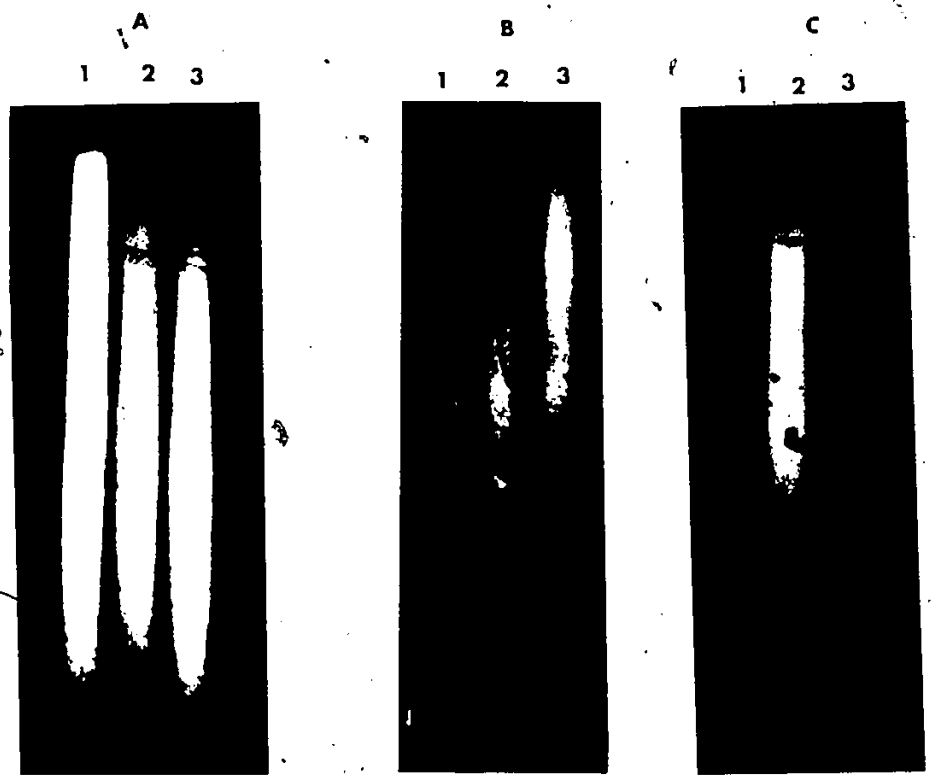

Figure 17

A Autoradiograph of northern blot hybridized with cDNA (3') to 229E RNA

Lane 1 229E RNA

Lane 2 Cell RNA

Lane 3 VH RNA

Each blot was pre-hybridized with calf thymus random primers and then hybridized with a cDNA (3') probe to 229E RNA.

B Autoradiograph of a northern blot hybridized with cDNA (3') to cellular RNA

Lane 1 229E RNA

Lane 2 Cell RNA

Lane 3 VH RNA

Each blot as pre-hybridized with calf thymus random primer and then hybridized with a cDNA (3') probe to cellular RNA.

C Autoradiograph of a northern blot hybridized with cDNA (3') to VH RNA

Lane 1 229E RNA

Lane 2 Cell RNA

Lane 3 VH RNA

Each blot was pre-hybridized with calf thymus random primer and then hybridized with a cDNA (3') probe to VH RNA.

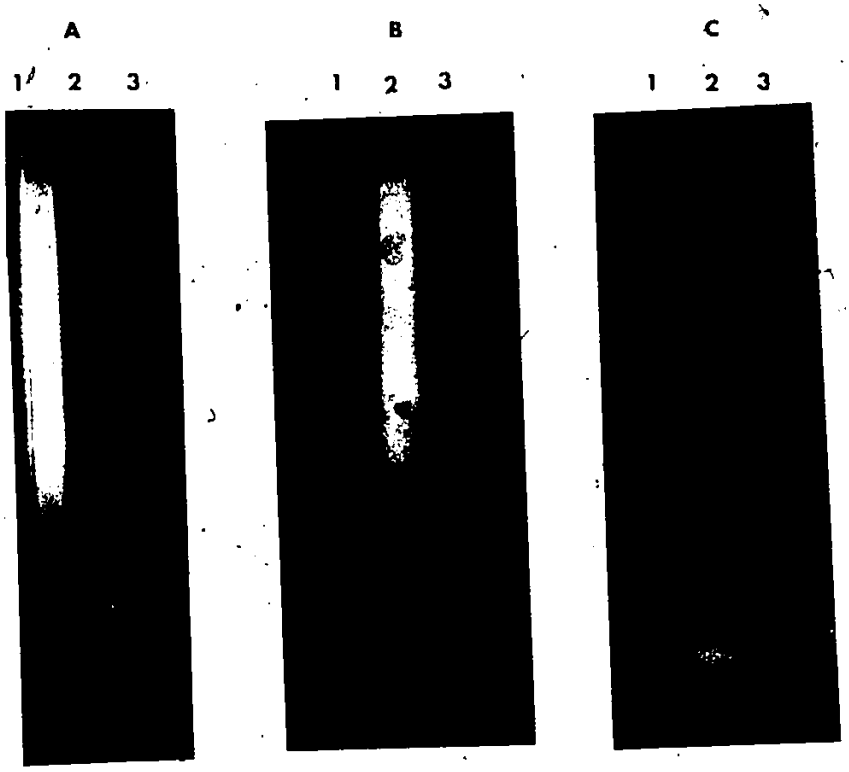
A
1 2 3
B
1 2 3
C
1 2 3

seen very clearly (Fig. 18 A). cDNA (3') to 229E RNA appeared to react more strongly with VH RNA than to 229E RNA, which may be an indication that the VH RNA is larger and thus a greater quantity of it remains in the gels after blotting. Only a weak reaction with cellular cRNA was found with cDNA (3') to cellular RNA and no reaction with 229E RNA or VH RNA (Fig. 18B).

Figure 18

A Autoradiograph of a northern blot hybridized with cDNA (3') to 229E RNA

The same gel as in Figure 17 was treated with NaOH to hydrolyze residual RNA, blotted and hybridized with cDNA (3') to 229E RNA.

B Autoradiograph of a northern blot hybridized with cDNA (3') to cellular RNA

The same gel as in Figure 17 was treated with NaOH to hydrolyze residual RNA, blotted and hybridized with cDNA (3') to cellular RNA.

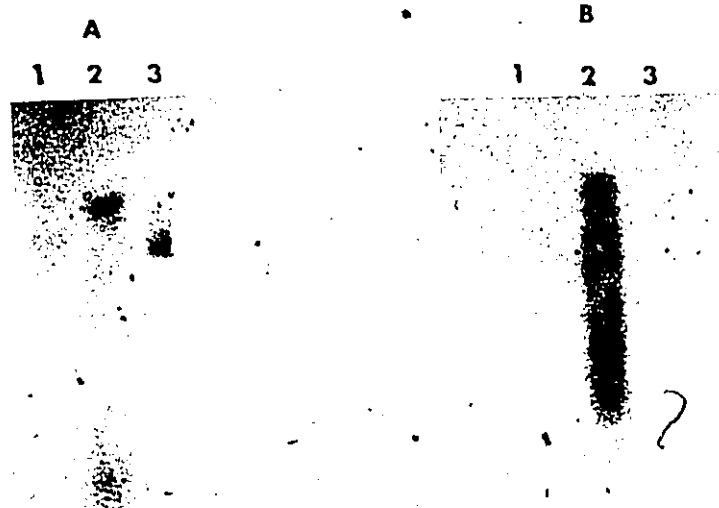
A
1 2 3
B
1 2 3

IV. DISCUSSION

This work represents a portion of a larger study to determine the mechanism of persistence and to characterize progeny persistent viruses. It had previously been found and reported that the parental human coronavirus strain 229E and the persistent VH strain derived from it had some differences in biological properties. The goal of the present work was to attempt to demonstrate genetic differences at the molecular level i.e. to establish that the differences were inherent properties of progeny virions. A number of established methods are available to do this.

One possibility was to study the proteins associated with each virus. Differences between the viruses might be reflected in differences in their proteins when electrophoresed or when separated by immunoprecipitation. Another possibility was to study the RNA genome of each virus. The RNA may be compared electrophoretically, by oligonucleotide fingerprinting and by hybridization. The latter was chosen to establish if any differences did exist within the genome of each virus.

To do this, cDNA was synthesized with RNA from each virus, and was used to compare the genomes of these strains. Rigorous attention to any possible source of RNase contamination was found to be critical in all aspects of these experiments.

The successful accomplishments of these experiments depended on the quality of the RNA. Initially, RNA was extracted from freeze-thawed preparations of virus-cell lysates. In all probability, large quantities of RNases, cellular RNA and DNA, and large amounts of protein made this source of virus less than ideal for preparation of RNA for use as template in cDNA syntheses. The clue to obtaining a 60S RNA band was to

use virus from the SNF of cultures of undegraded cells. This eliminated many of the unwanted components from the preparation.

Another factor which contributed significantly to the detection and isolation of 60S genomic RNA was the use of Act-D. By shutting off cellular RNA synthesis with Act-D, only viral RNA was able to incorporate the ^{3}H-uridine. Therefore fluorography of specific viral bands in gels was improved although the yield of infectious virus was 4-fold less in the SNF of Act-D treated cells at 40 hours post infection (4 x 106 pfu/mL). This was considered to provide adequate quantities of virus for these experiments.

This reduction in yield caused by Act-D is less than in previous studies on virus present in whole cell lysates, in which 50 to 100-fold reductions were found (Kennedy and Johnson-Lussenburg, 1979). However, since only infectious virus released into the SNF was used in this study, a direct comparison of these results is not appropriate, as the results in the previous study were obtained from whole cell lysates of frozen and thawed cultures.

The presence of Act-D in cultures was also slightly toxic at the 1 ug/mL level, as evidenced by cells detaching from the culture surface, but they appeared to maintain their integrity, and therefore very little soluble cellular material might be expected to be present in the SNF. The presence of Act-D ensured the preferential labelling of viral RNA, but it did not exclude the presence of unlabelled cellular RNA from the preparations. Therefore, host RNA contaminants were not eliminated, just markedly reduced. Further confirmation of the viral nature of the 60S RNA products depends on the fact that under these conditions, host RNA would not be found in the 60S size range.

The isolated 229E RNA and VH RNA were compared electrophoretically using 15% agarose gels. The viral RNA bands of each genome migrated in the range expected for 60S size RNA and it was repeatedly found that the mobility of the 229E RNA was slightly higher than the VH RNA. This indicated that the persistent progeny VH RNA was larger than the parental standard 229E RNA. This finding was surprising since it had been expected that the persistent VH RNA would be, if anything, smaller than the parental. Furthermore, the difference in mobilities indicated a significant difference in the genome sizes, the VH being 10-15% larger at least.

The question was whether additional viral sequences were included within the larger VH genome, or whether the size difference reflected incorporation of non-genome sequences. It must be remembered that whatever the case, the additional sequences not only did not interfere with viral replication, but enhanced it as increased infectious VH virus yields were obtained under lytic conditions at 33°C. Furthermore, the sequences may have played an important role in the initial establishment of the VH persistent infection.

Hybridization was the method selected to further characterize the differences between the VH and 229E genomes. The results of the liquid hybridization experiments using cDNA representative of the whole viral genomes confirm that there is a difference in the sequences of the VH and 229E genomes. Interpretation of these findings depends on the cDNA used, both as to the template RNA and the relative molar concentration of the cDNAs synthesized. In both systems [229E cDNA (rep.) and VH cDNA (rep.)] the differences between homologous and heterologous hybridizations indicated changes had occurred in the genome. It could be postu-

lated that the additional RNA sequences in the VH genome could be derived from either viral and/or host RNA. However the nature of the inserted sequences could not be determined from these results. Recently, differences have been revealed, between 229E and VH viruses by neutralization kinetics and by monoclonal fluorescent antibody analysis, which are associated with the E2 peplomer glycoprotein (Johnson-Lussenburg, unpublished results). On this basis it might also be postulated that some portion of the genomic difference might be located in the E2 mRNA region.

The results of northern blot hybridizations also reflected differences between the 229E and VH RNAs. $cDNA_{rep}$ to 229E and VH RNA would be expected to hybridize well with their homologous genome RNA as was observed in both systems. However, reaction also occurred with control cellular RNA in the 28S and lower size region, but not in the region of the 60S size RNA genome. This was interpreted as an indication that there might be host contaminating sequences in the viral RNA templates used to prepare cDNA. This would also explain the high background in liquid hybridization results between both VH and 229E cDNAs and host RNA.

The use of cDNA to the 3'-end of the genome (oligo-dT primed) would be expected to identify putative differences in the smallest mRNA sequences. This mRNA (7) codes for the N protein and is located in this region. In control experiments, cDNA (3') synthesized to cellular RNA reacted specifically with cellular RNA and not viral RNA. However, cDNA (3') to 229E RNA or VH RNA hybridized to low levels with cellular RNA, the reactions occurring in the region of 28S RNA or less. There can be several explanations for these results: (1) some cellular RNA may remain

in the viral template RNA used for synthesis; (2) host sequences may occur in the viral genome; or (3) this represents a preparation artifact due to the use of oligo-dT. The first explanation is the most likely but does not preclude the others. In fact all 3 may be involved to varying degrees.

If the smaller 229E RNA transferred more completely than the larger VH RNA, then a greater amount of 229E RNA would be present in the biodyne membrane which could result in a more intense reaction. Such a result could be misinterpreted as indicating differences in homologies. Therefore several experiments were designed to substantiate that both 60S RNAs had actually transferred from the agarose gel to the biodyne membrane.

Evaluation of gels pre- and post-blotting indicated that most of the smaller RNAs were rapidly transferred and that some but not all the larger 60S size RNAs blotted. By hydrolyzing the residual RNA in the gels and then re-blottng, it was possible to hybridize all the RNA. After hydrolysis, there was enough 60S RNA to hybridize to the cDNA synthesized to oligo-dT_{12-18}. This cDNA to the 3' end of the 229E RNA genome appeared to react more strongly with the VH RNA than to the 229E RNA in blot. This suggested that there was a less efficient transfer of the original VH RNA from the gel which when hydrolyzed was small enough to readily transfer to the membrane and to give the stronger reaction.

Equal amounts of each 60S RNA would have to be transferred in order to detect the same degree of hybridization with each cDNA. Although the amount of RNA was not evaluated quantitatively, the RNAs were transferred under identical conditions and should have transferred with

the same efficiency if they were exactly identical. If they were not identical, then the larger RNA would be expected to transfer with the least efficiency and would produce the results found.

When the results of the northern blots of $cDNA_{rep}$ and $cDNA_{3'}$ were compared it was apparent that greater differences were observed between the cDNA reactions that with those of the $cDNA_{3'}$. This implied that major differences between the two virus RNAs occur predominately upstream from the 3'-end. Whether single or multiple changes are involved cannot be deduced from these results.

Recently 6 differences were reported between the standard MHV-JHM and persistent non-syncytia forming Neuro-2A (JHM) which were located in the 5'-region of RNA-3, RNA-1 and RNA-2 (Leibowitz et al., 1984). Since it had already been demonstrated that RNA-3 coded for the precursor to glycoprotein E2 (Siddell et al., 1981), and others had implicated the E2 protein in MHV-induced cell fusion (Collins et al., 1982; Holmes and Behnke, 1981), it was suggested that the modification in the RNA-3 portion of the genome which codes for E2 might have resulted in the alteration in the syncytia-forming phenotype. It is tempting to speculate that a similiar change in the mRNA region of 229E coding for the E2 has occurred resulting in the VH virus with its characteristic phenotype. However, these results suggest more extensive changes have occurred.

V. CONCLUSIONS

A number of molecular differences have been found between the 229E RNA and the VH RNA genomes. By agarose gel electrophoresis, the 60S genomic RNA of 229E virus migrated faster than the 60S genomic RNA of persistent VH virus. It was concluded that the VH RNA was larger than the 229E RNA.

In liquid hybridization experiments, a 2 log difference in the 50% R_0t values was found using cDNA (rep.) synthesized with random primers and 229E RNA template.

When hybridized to completion with 229E cDNA (rep.), VH RNA is saturated at 67% of the value for 229E RNA. This represented a 33% difference between the 229E RNA and the VH RNA. When hybridized to completion with VH cDNA (rep.), 229E RNA was saturated at 86% of the homologous value.

Northern blot hybridization revealed a pattern of preferential hybridization for 229E RNA when cDNA (rep.) from random primer was used. Northern blots using cDNA (3') synthesized from oligo-dT primers representing only the 3'-end of the genome, did not reveal these differences so strongly. It was concluded that any changes in the RNA genome were not at the 3'-end.

These facts, when taken together indicated that there were molecular differences between the genomes of the parental human coronavirus 229E and the persistent VH strain derived from it, and that these differences are probably upstream from the 3'-end of the genome.

FUTURE RESEARCH

One area of further research could address the question of where

specifically have change(s) occurred in the HCV 229E genome. A change in the genome would be reflected in one of the mRNAs which in turn should be reflected in the protein translated from it. If 229E and VH mRNAs were isolated from infected cells by gel electrophoresis, they could be used for in vitro translation in the rabbit reticulocyte system for non-glycosylated proteins and in Xenopus laevis (frog) oocytes for glycosylated proteins (Pelham and Jackson, 1976). The translation products could be characterized and identified using polyclonal and monoclonal antibodies which are available to 229E virus. A difference in the E1 or E2 protein, for example, may be reflected in a difference in electrophoretic mobility. Using the Western blot technique the different protein bands could be identified. Immunoprecipitation would allow the isolation of the specific protein. At this point the mRNA containing a change in its RNA should be identified (Leibowitz et al., 1984).

In order to estimate the number of changes in the mRNA and the genome RNA, oligonucleotide fingerprints using T_1-ribonuclease could be prepared. Other studies have found this procedure very sensitive in detecting minor differences (Clewley et al., 1981). In a set of mouse coronaviruses, very similar to the 229E and VH human coronaviruses, at least 6 differences were found in oligonucleotide patterns between standard MHV-JHM and the persistent strain Neuro-2A (JHMV) (Leibowitz et al., 1984). Any unique oligonucleotide spots could be eluted and used for cloning studies.

Once it had been established which mRNA or oligonucleotide spots were of interest, the RNA could be cloned using pBR322 (Lavi et al., 1984). This would yield large quantities of readily available cDNA

which could be nick-translated and used for hybridization and sequencing. One of the hinderences in the present work was the very small (nanogram) quantities of cDNA available for experiments. Cloning would overcome this problem.

The availability of cloned cDNA would permit heteroduplex mapping with plasmids with the electron microscope (Evenson, 1977). This would reveal differences, by a direct means, as seen by loops of non-hybridization.

Finally, cloned cDNA would allow in situ hybridization studies which could detect the presence of VH RNA in the persistently infected HV cells. There is still an open question as to the association of human coronavirus with multiple sclerosis. In situ hybridization could be used to examine specimens from multiple sclerosis patients (Lavi et al., 1984). If these results should be positive, it would answer the question once and for all, and greatly advance the knowledge and hopefully treatment and prevention of this disease.

VI. REFERENCES

ALWINE, J.C., KEMP, D.J., and STARK, G.R. 1977. Method for detection of specific RNAs in agarose gels by transfer to diazobenzyloxymethyl paper and hybridization with DNA probes. Proc. Natl. Acad. Sci. USA 74, 5350-5354.

ANDRIES, K., and PENSAERT, M.B. 1980a. Virus isolation and immunofluorescence in different organs of pigs infected with hemagglutinating encephalitis virus. Am. J. Vet. Res. 41, 215-218.

ANDRIES, K., and PENSAERT, M.B. 1980b. Immunofluorescence studies on the pathogenesis of hemagglutinating encephalomyelitis virus infection in pigs after oronasal infection. Am. J. Vet. Res. 41, 1372-1378.

ANDRIES, K., PENSAERT, M.B., and CALLEBAUT, P. 1978. Pathogenicity of hemagglutinating encephalomyelitis (vomiting and wasting disease) virus of pigs, using different routes of inoculation. Zentrl. Vet. 25, 461-468.

BARILE, M.F., and KERN, J. 1971. Isolation of Mycoplasma arginini from commercial bovine sera and its implication in contaminated cell cultures. Proc. Soc. Biol. Med. 138, 432-437.

BEESLEY, J.E., and HITCHCOCK, L.M. 1982. The ultrastructure of feline infectious peritonitis virus in feline embryonic lung cells. J. Gen. Virol. 59, 23-28.

BHATT, P.N., and JACOBY, R.C. 1977. Experimental infection of adult axenic rats with Parker's rat coronavirus. Arch. Virol. 54, 345-352.

BOND, C.W., ANDERSON, K., and LEIBOWITZ, J.L. 1984. Protein synthesis in cells infected by murine hepatitus viruses JHM and A59: tryptic peptide analysis. Arch. Virol. 80, 333-347.

BONNER, T.I., and LASKEY, R.A. 1974. A film detection method for tritium labelled proteins and nucleic acids in polyacrylamide gels. European J. Biochem. 46, 83.

BRADBURNE, A.F., and TYRRELL, D.A.J. 1969. The propagation of coronaviruses in tissue culture. Arch. Virol. 28, 133-150.

BRAYTON, P.R., GANGES, R.G., and STOHLMAN, S.A. 1981. Host cell nuclear function and murine hepatitis virus replication. J. Gen. Virol. 56, 457-460.

BRAYTON, P.R., LAI, M.M.C., PATTON, C.D., and STOHLMAN, S. 1982. Characterization of two RNA polymerase activities induced by mouse hepatitis virus. J. Virol. 42, 847-853.

BRIAN, D.A., DENNIS, D.E., and GUY, J.S. 1980. Genome of porcine transmissible gastroenteritis virus. J. Virol. 34, 410-415.

BRITTEN, R.J., GRAHAM, R.J., and NEUFELD, B.R. 1974. Analysis of repeating DNA sequences by re-association. Meth. Enzymol. 29, 363-405.

BURKS, J.S., DEVALD, B.L., JANKOVSKY, L.D., and GERDES, J.C. 1980. Two coronaviruses isolated from central nervous system tissue of two multiple sclerosis patients. Science 209, 933-934.

CARTHEW, P., and SPARROW, S. 1981. Murine coronaviruses: the histopathology of disease induced by intranasal inoculation. Res. Vet. Sc. 30, 270-273.

CAUL, E.O., ASHLEY, C.R., FERGUSON, M., and EGGLESTONE, S.J. Preliminary studies on the isolation of coronavirus 229E nucleocapsids. FEMS Microb. Letters 5, 101-105.

CHALONER-LARSSON, G. and JOHNSON-LUSSENBURG, C.M. 1981a. Characterization of a long term in vitro persistent infection with human coronavirus 229E. Adv. Exp. Med. Biol. 142, 309-322.

CHALONER-LARSSON, G., and JOHNSON-LUSSENBURG, C.M. 1981b. Establishment and maintenance of a persistent infection of L132 cells by human coronavirus strain 229E. Arch. Virol. 69, 117-129.

CHELEY, S., and ANDERSON, R. 1981. Cellular synthesis and modification of murine hepatitis virus polypeptides. J. Gen. Virol. 54, 301-311.

CHELEY, S., ANDERSON, R., CUPPLES, M.J., LEE CHAN, E.C.M., and MORRIS, V.L. 1981a. Intracellular murine hepatitis virus-specific RNAs contain common sequences. Virol. 112, 596-604.

CHELEY, S., MORRIS, V.L., CUPPLES, M.J., and ANDERSON, R. 1981b. RNA and polypeptide homology among murine coronaviruses. Virol. 115, 310-321.

CLEWLEY, J.P., MORSER, J., AVERY, R.J. and LOMNICZI, B., 1981. Oligonucleotide fingerprinting of the RNA of different strains of infectious bronchitis virus. Infect. Immun. 32, 1227-1233.

COLLINS, A.R., KNOBLER, R.L., POWELL, H., and BUCHMEIER, M.J. 1982. Monoclonal antibodies to murine hepatitis virus 4 (strain JHM) define the viral glycoprotein responsible for attachment and cell fusion. Virol. 119, 358-371.

DAVIES, H., DOURMASHKIN, R.R., and MACNAUGHTON, M.R. 1981. Ribonucleoprotein of avian infectious bronchitis virus. J. Gen. Virol. 53, 67-74.

DAVIS, E.V., and BOLIN, V.S. 1960. Fed. Proc. 19, 386.

DOUGHRI, A.M., and STORZ, J. 1977. Light and ultrastructural pathologic changes in intestinal coronavirus infection in newborn calves. Zentralblatt fur Veterin. 24, 367-385.

DUCATELLE, R., COUSSEMENT, W., PENSAERT, M.B., DEBOUCH, P., and HOORENS, J. 1981. In vitro morphogenesis of a new porcine enteric coronavirus CV777. Arch. Virol. 68, 35-44.

EVENSON, D.P., 1977. Electron microscopy of viral nucleic acids, pp 219-264. In: Methods in Virology, Eds. K. Maramorosch & H. Koproioski. Acad. Press Inc.

FEDORCSAK, I., and EHRENBERG, L. 1966. Effects of diethyl-pyrocarbonte and methyl methane sulfonate on nucleic acids and nucleases. Acta Chem. Scand. 20, 107.

FLEURY, H.J.A., SHEPPARD, M.B., and RAINE, C.S. 1980. Further ultrastructural observations of virus morphogenesis and myelin pathology in JHM virus encephalomyelitis. Neuropathol. Appl. Neurobiol. 6, 165-169.

FRIEDMAN, R.M., and RAMSEUR, J.M. 1979. Mechanisms of persistent infections by cytopathic viruses in tissue culture. Arch. Virol. 60, 83-103.

GARLINGHOUSE, L.E., SMITH, A.L., and HOLFORD, T. 1984. The biological relationships of mouse hepatitis virus (MHV) strains and interferon: in vitro induction and sensitivities. Arch. Virol. 82, 19-29.

GARWES, D.J., and POCOCK, D.H. 1975. The polypeptide structure of transmissible gastroenteritis virus. J. Gen. Virol. 29, 25-34.

GARWES, D.J., POCOCK, D.H., and WIJASKZA, T.M. 1975. Identification of heat-dissociable RNA complexes in two porcine coronaviruses. Nature (London). 257, 508-510.

GERNA, G., CEREDA, P.M., REVELLO, M.G., CATTANEO, E., BATTAGLIA, M., and TORSELLINI-GERNA, M. 1981. Antigenic and biologic relationships between human coronavirus OC43 and neonatal calf diarrhea coronavirus. J. Gen. Virol. 54, 91-102.

GLISIN, V., KRKUENJAKOV, R., and BYUS, C. 1974. Ribonucleic acid isolated by cesium chloride centrifugation. Biochem. 13, 2633-2637.

HAASE, A.T., VENTURA, P., JOHNSON, K.P., NORRBY, E., and GIBBS, C.J. 1981. Measles virus infection of the central nervous system. J. Infect. Dis. 144, 154-160.

HAMRE, D., and PROCKNOW, J.J. 1966. A new virus isolated from the human respiratory tract. Proc. Soc. Exp. Biol. 121, 190-193.

HAMRE, D., KINDIG, D.A., and MAN, J. 1967. Growth and intracellular development of a new respiratory virus. J. Virol. 1, 810-816.

HASONY, H.J., and MACNAUGHTON, M.R. 1981. Antigenicity of mouse hepatitis virus type 3 subcomponents in C57 strain mice. Arch. Virol. 69, 33-41.

HASONY, H.J., and MACNAUGHTON, M.R. 1982. Serological relationships of the subcomponents of human coronavirus strain 229E and mouse hepatitis virus strain 3. J. Gen. Virol. 58, 449-452.

HASPEL, M.V., LAMPERT, P.W., and OLDSTONE, M.B.A. 1978. Temperature-sensitive mutants of mouse hepatitis virus produce a high incidence of demyelination. Proc. Natl. Acad. Sci. USA 75, 4033-4036.

HELENIUS, A., FRIES, E., GAROFF, H., and SIMONS, K. 1980. On the entry of Semliki Forest virus into BHK-21 cells. J. Cell. Biol. 84, 404-420.

HERNDON, R.M., GRIFFIN, D.E., MCCORMICK, U., and WEINER, L.P. 1975. Mouse hepatitis virus recurrent demyelination. Arch. Neurol. 32, 32-35.

HIATT, H.H. 1962. A rapidly labeled RNA in rat liver nuclei. J. Molec. Biol. 5, 217-228.

HIERHOLZER, J.C., BRODERSON, J.R., and MURPHY, F.A. 1979. New strain of mouse hepatitis virus as the cause of lethal enteritis in infant mice. Infect. Immun. 24, 508-522.

HIRANO, N., GOTO, N., MAKINO, S., and FUJIWARA, K. 1981. Persistent infection with mouse hepatitis virus JHM in DBT cell culture. In: Biochemistry and Biology of Coronaviruses. ter Meulen, V., Siddell, S., and Wege, H. (eds.). (Adv. Exp. Biol. Med., Vol. 142), 301-308. Plenum Press, N.Y.

HOLLAND, J.J., VILLAREAL, L.P., WELSH, R.M., OLDSTONE, M.B.A., KOHNE, D., LAZZARINI, R., and SCOLNICK, E. 1976. Longterm persistent VSV and rabies virus infection of cells in vitro. 33, 193-211.

HOLMES, K.V., DOLLER, E.W., and STURMAN, L.S. 1981. Tunicamycin resistant glycosylation of a coronavirus glycoprotein: demonstration of a novel type of viral glycoprotein. Virol. 115, 334-344.

HOLMES, K.V., and BEHNKE, J.N. 1981. Evolution of a coronavirus during persistent infection in vitro. In: Biochemistry and Biology of Coronaviruses. ter Meulen, V., Siddell, S., and Wege, H. (eds.). (Adv. Exp. Biol. Med. Vol. 142), pp 287-299. Plenum Press, N.Y.

HORZINEK, M.C., LUTZ, H., and PEDERSEN, N.C. 1982. Antigenic relationships among homologous structural polypeptides of porcine, feline and canine coronaviruses. Infect. Immun. 37, 1148-1155.

HUANG, A.S., and BALTIMORE, D. 1977. Defective interfering animal viruses. Comp. Virol. 10, 73-116.

JACOBS, L., SPAAN, W.J.M., HORZINEK, M.C., and VAN DER ZEIJST, B.A.M. 1981. The synthesis of the subgenomic mRNAs of mouse hepatitis virus is initiated independently: evidence from UV transcriptional mapping. J. Virol. 39, 401-406.

KEMP, M.C., HEIRHOLZER, J.C., HARRISON, A., and BURKS, J.S. 1984. Characterization of viral proteins synthesized in 229E infected cells and Effect(s) of inhibition of glycosylation and glycoprotein transport. Adv. Exp. Biol. Med. 173, 65-77.

KENNEDY, D.A., and JOHNSON-LUSSENBURG, C.M. 1975/76. Isolation and morphology of the internal component of human coronavirus strain 229E. Intervirol. 6, 197-206.

KENNEDY, D.A. 1976. Studies on the biology of a human coronavirus. Ph.D. Thesis, University of Ottawa, Ottawa, Ont.

KENNEDY, D.A., and JOHNSON-LUSSENBURG, C.M. 1979. Inhibition of coronavirus 229E replication by actinomycin-D. J. Virol. 29, 401.

KIRBY, K.S. 1956. A new method for the isolation of nucleic acids from mammalian tissues. Biochem. J. 64, 405.

KOOLEN, M.J.M., OSTERHAUS, A.D.M.E., SIEBELINK, K.H.J., HORZINEK, M.C., and VAN DER ZEIJST, B.A.M. 1984. Monoclonal antibodies to the three classes of mouse hepatitis virus strain A59 proteins. Adv. Exp. Med. Biol. 173, 115-116.

KRZYSTYNIAK, K., and DUPUY, J.M. 1981. Early interaction between mouse hepatitis virus 3 and cells. J. Gen. Virol. 57, 53-61.

LAI, M.M.C., and STOHLMAN, S.A. 1978. The RNA of mouse hepatitis virus. J. Virol. 26, 236-242.

LAI, M.M.C., and STOHLMAN, S.A. 1981b. Genome structure of mouse hepatitis virus. Comparative analysis by oligonucleotide mapping. Adv. Exp. Med. Biol. 142, 69-82.

LAI, M.M.C., PATTON, C.D., and STOHLMAN, S.A. 1982a. Further characterization of mRNAs of mouse hepatitis virus: presence of common 5'-end nucleotides. J. Virol. 41, 557-565.

LAI, M.M.C., PATTON, C.D., and STOHLMAN, S.A. 1982b. Replication of mouse hepatitis virus: negative-stranded RNA and replicative form RNA are of genome length. J. Virol. 44, 487-492.

LAI, M.M.C., FLEMING, J.O., STOHLMAN, S.A., and FUJIWARA, K. 1983. Genetic heterogeneity of murine coronaviruses. Arch. Virol. 78, 167-175.

LAI, M.M.C., BARIC, R.S., BRAYTON, P.R., and STOHLMAN, S. 1984. Studies on the mechanism of RNA synthesis of a murine coronavirus. Adv. Exp. Med. Biol., 173, 187-200.

LAMPERT, P.W., SIMS, J.K. and KNIAZEFF, A.J. 1973. Mechanism of demyelination in JHM virus encephalomyelitis. Electron microscopy studies. Acta Neuropathol. 24, 76-85.

LAVI, E., GILDEN, D.H., HIGHKIN, M.K., and WEISS, S.R. 1984. Persistence of mouse hepatitis virus A59 RNA in a slow virus demyelinating infection in mice as detected by in situ hybridization. J. Virol. 51, 563-566.

LEIBOWITZ, J.L., and WEISS, S.R. 1981. Murine coronavirus RNA. Adv. Exp. Biol. Med. 142, 227-244.

LEIBOWITZ, J.L., WILHELMSEN, K.C., and BOND, C.W. 1981. The virus-specific intracellular RNA species of two murine coronaviruses: MHV-A59 and MHV-JHM. Virol. 114, 29-51.

LEIBOWITZ, J.L., WEISS, S.R., PAAVOLA, E., and BOND, C.W. 1982. Cell-free translation of coronavirus RNA. J. Virol. 43, 905-913.

LEIBOWITZ, J.L., BOND, C.W., ANDERSON, K., and GOSS, S. 1984. Biological and Macromolecular Properties of Murine Cells Persistently Infected with JHM-MHV. Arch. Virol. 80, 315-332.

LOMNICZI, B., and KENNEDY, I. 1977. Genome of infectious bronchitis virus. J. Virol. 24, 99-107.

LUCAS, A., FLINTOFF, W., ANDERSON, R., PERCY, D., COULTER, M., and DALES, S. 1977. In vivo and in vitro models of demyelinating disease: tropism of JHM strain of mouse hepatitis virus for cells of glial origin. Cell. 12, 553-560.

LUCAS, A., COULTER, M., ANDERSON, R., DALES, S., and FLINTOFF, W. 1978. In vivo and in vitro models of demyelinating diseases: persistence and host-regulated thermosensitivity in cells of neural derivation infected with mouse hepatitis and measles viruses. Virol. 88, 325-337.

MACNAUGHTON, M.R., and MADGE, H.M. 1977. The characterization of the virion RNA of avian infectious bronchitis virus. FEBS Lett. 77, 311-313.

MACNAUGHTON, M.R., and MADGE, H.M. 1978. The genome of human coronavirus strain 229E. J. Gen. Virol. 39, 497-504.

MACNAUGHTON, M.R., DAVIES, H.A., and NERMUT, M.V. 1978. Ribonucleoprotein-like structures from coronavirus particles. J. Gen. Virol. 39, 545-549.

MACNAUGHTON, M.R. 1981. Structural and antigenic relationships between human, murine and avian coronaviruses. Adv. Exp. Biol. Med. 142, 19-28.

MACNAUGHTON, M.R., MADGE, H.M., and REED, S.E. 1981. Two antigenic groups of coronaviruses detected by using enzyme-linked immunosorbent assay. Infect. Immun. 33, 734-737.

MAHY, B.W.J., SIDDELL, S., WEGE, H., and TER MEULEN, V. 1983. RNA-dependent RNA polymerase activity in murine coronavirus-infected cells. J. Gen. Virol. 64, 103-111.

MALLUCI, L. 1965. Observations on the growth of mouse hepatitis virus (MHV-3) in mouse macrophages. Virol. 25, 30-37.

MANIATIS, T., FRITSCH, E.F., and SAMBROOK, J. 1980. Molecular cloning, a laboratory manual. Cold Spring Harbor.

MARU, M., and SATO, K. 1982. Characterization of a coronavirus isolated from rats with sialoadenitis. Arch. Virol. 73, 33-43.

MASSALSKI, A., COULTER-MACKIE, M., and DALES, S. 1981. Assembly of mouse hepatitis virus strain JHM. Adv. Exp. Biol. Med. 142, 111-118.

MASSALSKI, A., COULTER-MACKIE, M., and DALES, S. 1982. In vivo and in vitro models of demyelinating diseases. V. Comparison of the assembly of mouse hepatitis virus, strain JHM, in two murine cell lines. Intervirol. 18, 135-146.

MCMASTER, G.K., and CARMICHAEL, G.G. 1977. Analysis of single- and double-stranded nucleic acids on polyacrylamide and agarose gels using glyoxal and acridine orange. Proc. Soc. Natl. Sci. USA 74, 4835-4838.

MEINKOTH, J., and WHAL, G. 1984. Hybridization of nucleic acids immobilized on solid supports. Anal. Biochem. 138, 267-284.

MONTO, A.S., and RHODES, L.M. 1977. Detection of coronavirus infection of man by immunofluorescence. Proc. Soc. Exp. Biol. Med. 155, 143-148.

NIEMANN, H., and KLENK, H.D. 1981a. Glycoprotein E1 of Coronavirus A59. A new type of viral glycoprotein. Adv. Exp. Biol. Med. 142, 119-131.

NIEMANN, H., and KLENK, H.D. 1981b. Coronavirus glycoprotein E1, a new type of viral glycoprotein. J. Mol. Biol. 153, 993-1010.

NIEMANN, H., BOSCHEK, B., EVANS, D., ROSING, M., TAMURA, T., and KLENK, H.D. 1982. Subcellular localization of the post-translational glycosylation of coronavirus glycoprotein E1. EMBO J. 1, 1499-1504.

NISHIYAMA, Y. 1977. Studies of L cells persistently infected with VSV: factors involved in the regulation of persistent infection. J. Virol. 35, 265-279.

PARKER, J.S., CROSS, S.S., and ROWE, W.P. 1970. Rat coronavirus, a prevalent, naturally-occurring pneumotropic virus of rats. Arch. Virol. 31, 293-302.

PATTERSON, S., and MACNAUGHTON, M.R. 1981. The distribution of the human coronavirus 229E on the surface of human diploid cells. J. Gen. Virol. 53, 267-273.

PEDERSON, N.C., WARD, J., and MENGELING, W.L. 1978. Antigenic relationship of the feline infectious peritonitis virus to coronaviruses of other species. Arch. Virol. 58, 45-53.

PELHAM, H.R.B., and JACKSON, R.J. 1976. An efficient mRNA-dependent translation system from reticulocyte lysates. Eur. J. Biochem. 67, 247-256.

PENSEART, M.B., DE BOUCK, P., and REYNOLDS, D.J. 1981. An immune electron microscopic and immunofluorescent study on the antigenic relationship between the coronavirus-like agent, CV777, and several coronaviruses. Arch. Virol. 68, 45-52.

PERRY, R.P., LATORRE, J., KELLY, D.E., and GREENBURG, J.R. 1972. On the lability of poly(A) sequences during extraction of mRNA from polyribosomes. Biochim. Biophys. Acta 262, 220-226.

PIKE, B.V.M, and GARWES, D.J. 1977. Lipids of transmissible gastroenteritis virus and their relation to those of two different host cells. J. Gen. Virol. 34, 531-535.

PREBLE, O.T., and YOUNGER, J.S. 1975. Temperature sensitive mutany viruses and the etiology of chronic and inapparent infections. J. Infect. Dis. 131, 467-473.

REYNOLDS, D.J., GARWES, D.J., and LUCEY, S. 1980. Differentiation of canine coronavirus and porcine transmissible gastroenteritis virus by neutralization with canine, porcine and feline sera. Vet. Microb. 5, 283-290.

RIMA, B.K., DAVIDSON, W.B. and MARTIN, S.J. 1977. The role of defective interfering particles in persistent infection of vero cells by measles virus. J. Virol. 35, 89-97.

ROTTIER, P.J.M., SPAAN, W.J.M., HORZINEK, M., and VAN DER ZEIJST, B.A.M. 1981. Translation of three mouse hepatitis virus (MHV-A59) subgenomic RNAs in Xenopus laevis oocytes. J. Virol. 38, 20-26.

ROTTIER, P., BRANDENBURG, D., ARMSTRONG, J., VAN DER ZEIJST, B., and WARREN, G. 1984. Assembly in vitro of a spanning membrane protein of the endoplasmic reticulum: the E1 glycoprotein of coronavirus mouse hepatitis virus A59. Proc. Natl. Acad. Sci. USA 81, 1421-1425.

SCHMIDT, O.W., and KENNEY, G.E. 1981. Immunogenicity and antigenicity of human coronavirus 229E and OC43. Infect. Immun. 32, 1000-1006.

SCHMIDT, O.W., and KENNEY, G.E. 1982. Polypeptides and functions of antigens from human coronaviruses 229E and OC43. Infect. Immun. 35, 515-522.

SCHOCHETMAN, G., STEVENS, R.H., and SIMPSON, R.W. 1977. Presence of infectious polyadenylated RNA in the coronavirus avian infectious bronchitis virus. Virol. 7, 772-782.

SIDDELL, S., WEGE, H., BARTHEL, A., and TER MEULEN, V. 1981. Intracellular protein synthesis and the in vitro translation of coronavirus JHM RNA. In: Biochemistry and Biology of Coronaviruses, Adv. Exp. Biol. and Med. 142, 193-207.

SIDDELL, S.G., ANDERSON, R., CAVANAUGH, D., FUJIWARA, K., KLENK, H.D., MACNAUGHTON, M.R., PENSAERT, M., STOHLMAN, S.A., STURMAN, L., and VAN DER ZEIJST, B.A.M. 1983. Coronaviridae. Intervirol. 20, 181-189.

SIDDELL, S., WEGE, H., and TER MEULEN, V. 1983. The biology of coronaviruses. J. Gen. Virol. 64, 761-776.

SNYDER, D.B., and MARQUARDT, W.W. 1984. Use of monoclonal antibodies to assess antigenic relationships of avian infectious bronchitis virus serotypes in the United States. Adv. Exp. Med. Biol. 173, 109-114.

SPAAN, W.J.M., ROTTIER, P.J.M., HORZINEK, M.C., and VAN DER ZEIJST, B.A.M. 1981. Isolation and identification of virus specific mRNAs in cells infected with mouse hepatitis virus (MHV-A59). Virol. 108, 424-434.

SPAAN, W.J.M., ROTTIER, P.J.M., HORZINEK, M.C., and VAN DER ZEIJST, B.A.M. 1982. Sequence relationships between the genome and the intracellular RNA species 1, 3, 6 and 7 of mouse hepatitis strain A59. J. Virol. 42, 432-439.

STERN, D.F., and KENNEDY, S.I.T. 1980a. Coronavirus multiplication strategy. I. Identification and characterization of virus-specified RNA. J. Virol. 34, 665-674.

STERN, D.F., and KENNEDY, S.I.T. 1980b. Coronavirus multiplication strategy. II. Mapping the avian infectious bronchitis virus intracellular RNA species to the genome. J. Virol. 36, 440-449.

STERN, D.F., and SEFTON, B.M. 1982. Coronavirus proteins: biogenesis of avian infectious bronchitis virus virion proteins. J. Virol. 44, 794-803.

STERN, D.F.M., and SEFTON, B.M. 1984. Coronavirus multiplication: locations of genes for virion proteins on the avian infectious brochitis virus genome. J. Virol. 50(1), 22-29.

STOHLMAN, S.A., and FRELINGER, J.A. 1978. Resistance to fatal central nervous system disease by mouse hepatitis strain JHM. I. Genetic analysis. Immunogenetics 6, 277-281.

STOHLMAN, S.A., and WEINER, L.P. 1978. Stability of neurotropic mouse hepatitis virus (JHM strain) during chronic infection of neuroblastoma cells. Arch. Virol. 57, 53-61.

STOHLMAN, S.A., SAKAGUCHI, A.Y., and WEINER, L.P. 1979. Characterization of the cold sensitive murine hepatitis virus mutants rescued from latently infected cells by cell fusion. Virol. 98, 448-455.

STURMAN, L.S., HOLMES, K.V., BEHNKE, J. 1980. Isolation of coronavirus envelope glycoproteins and interaction with viral nucleocapsid. J. Virol. 33, 449-454.

STURMAN, L.S., and HOLMES, K.V. 1983. The molecular biology of coronaviruses. Adv. Virus Res. 28, 35.

STURMAN, L.S., and HOLMES, K.V. 1984. Proteolytic cleavage of peplomeric glycoprotein E2 of MHV yields two 90K subunits and activates cell fusion. Adv. Exp. Biol. Med. 173, 25-35.

SZYBALSKI, E.H., and SZYBALSKI, W. 1979. (no title available) Gene. 7, 217-220.

TANNOCK, G.A. 1973. The nucleic acid of infectious bronchitis virus. Arch. Virol. 43, 259-271.

TANNOCK, G.A., and HIERHOLZER, J.C. 1977. The RNA of human coronavirus OC43. Virol. 78, 500-510.

TER MEULEN, V., SIDDELL, S., and WEGE, H. (eds.). 1981. Biochemistry and biology of the coronaviruses. Plenum Press, N.Y.

THOMAS, P.S. 1980. Hybridization of denatured RNA and small DNA-fragments transferred to nitrocellulose. Proc. Soc. Natl. Acad. Sci. USA 77, 5201-5205.

TYRRELL, D.A.J., ALMEIDA, J.D., BERRY, D.M., CUNNINGHAM, C.H., HAMRE, D., HOFSTAD, M.S., MALLUCI, L., and MCINTOSH, K. 1968. Coronaviruses. Nature (Lond.). 220, 650.

VALOTAIRE, Y., TENNISWOOD, M., LEGUELLEC, C., and TATA, J.R. 1984. The preparation and characterization of vitellogenin mRNA from Rainbow trout (Salmo gairdneri). Biochem. 217, 73-77.

WATKINS, H., REEVE, P., and ALEXANDER, D.J. 1975. The ribonucleic acid of infectious bronchitis virus. Arch. Virol. 47, 279-286.

WECKER, E., HUMMELER, K., and GOETZ, T. 1962. Relationship between viral RNA of MHV. Virol. 17, 110-117.

WEGE, H., MULLER, A., and TER MEULEN, V. 1978. Genomic RNA of the murine coronavirus JHM. J. Gen. Virol. 41, 217-227.

WEGE, H., SIDDELL, S., STURM, M., and TER MEULEN, V. 1981a. Coronavirus JHM: characterization of intracellular viral RNA. J. Gen. Virol. 54, 213-217.

WEGE, H., SIDDELL, S., STURM, M., and TER MEULEN, V. 1981b. Characterization of the viral RNA in cells infected with the murine coronavirus JHM. Adv. Exp. Med. Biol. 142, 91-101.

WEGE, H., SIDDELL, S., STURM, M., and TER MEULEN, V. 1981c. Genetic variation of neurotropic and non-neurotropic murine coronaviruses. J. Gen. Virol. 54, 67-74.

WEGE, H., SIDDELL, S. and TER MEULEN, V. 1982. The biology and pathogenesis of coronaviruses. Curr. Topics in Microb. and Immunol., 99, 165-200.

WEGE, H., KOGA, M., WATANABE, R., NAGASHIMA, K., and TER MEULEN, V. 1983. Neurovirulence of murine coronavirus JHM temperature-sensitive mutants in rats. Infect. Immun. 39, 1316-1324.

WEISS, R.C., and LEIBOWITZ, J.L. 1981. Comparison of the RNAs of murine and human coronaviruses. In: Biochemistry and Biology of Coronaviruses. ter Meulen, V., Siddell, S., Wege, H. (eds.). Plenum Press, N.Y., pp 245-260.

WEISS, R.C.,and LEIBOWITZ, J.L. 1983. Characterization of murine coronavirus RNA with virus-specific cDNA probes. J. Gen. Virol. 64, 127-133.

WILHELMSEN, K.C., LEIBOWITZ, J.L., BOND, C.W., and ROBB, J.A. 1981. The replication of murine coronaviruses in enucleated cells. Virol. 110, 225-230.

YASSEEN, S.A., and JOHNSON-LUSSENBURG, C.M. 1981. Antigenic studies on coronaviruses. I. Identification of the structural antigens of human coronavirus strain 229E. Can. J. Microb. 27, 334-342.

YOSHIKURA, H., and TEJIMA, S. 1981. Role of protease in the mouse hepatitis virus-induced cell fusion. Virol. 113, 503-511.

ZHANDOV, V.M. 1975/1976. Integration of genomes of infectious RNA viruses. Intervirol. 6, 128-132.

APPENDIX I

SUPPLIERS OF MATERIALS AND EQUIPMENT

Amicon, Lexington, MA, USA
- ultra filtration cells and supplies

Beckman, Canada, Ottawa
- micropipettors and supplies
- ultracentrifuge and microfuge
- ultracentrifuge heads
- scintillation counter
- aquasol scintillaton fluid

Bio Rad, USA
- AG 501-x8 mixed bed resin
- Gel Dryer
- electrophoresis apparatus

Fisher, Canada, Ottawa
- disposable pipets and related disposable and non-disposable glassware
- NaCl, $NaHCO_3$, toluene
- 8 - hydroxy quinoline
- glyoxal
- dimethy sulfoxide (DMSO)
- microfuge and heads
- Tris buffer
- other miscellaneous chemicals

Flow Laboratories, Inc., Mississauga, ON
- Minimum Essential Medium (MEM)
- Fetal calf serum
- Medium 199 (M199)
- Glutamine

Gilson, Toronto, ON
- micropipettors and supplies

Ilford Ltd., Basildon, Essex, England
- film (FP4)

International Equipment Co., Fisher Scientific
- centrifuge and heads

Kodak, Toronto, ON
- XAR Film
- photographic chemicals
- diethylpyrocarbonate (DEP)
- film cassettes

Life Sciences Inc., Florida, USA
- avian myecloblastosis virus reverse transcriptase

LKB, Uppsalla, Sweden
- peristaltic pump

Lux Scientific, Mississauga, ON
- tissue culture flasks
- other related plastics for tissue culture

Miles Laboratories Ltd., USA
- *E. coli* RNA
- DNA

Millipore-Inc.
- filter apparatus and filters

New England Nuclear, Boston, MA, USA
- diphenyloxazole (PPO)
- radioisotopes ^{3}H-uridine
- 5'- ^{32}P-deoxycytosine triphosphate
- restriction enzymes

Oxoid Canada, Ottawa, ON
- Ion agar No. 1

PALL, Brockville, ON
- biodyne membranes

Polaroid, Mississauga, ON
- MP3 camera
- film

Schwarz-Mann
- Actinomycin D

Sigma, St. Louis, MI, USA
- agarose
- bromo deoxyuridine (BUDR)
- DEAE (diethyl-amino-ethyl)-dextran
- oligo-dT cellulose, oligo-dT_{12-18}
- penicillin, streptomycin, neomycin, kanamycin

APPENDIX II

ANALYSIS OF LIQUID HYBRIDIZATION REACTIONS

The kinetic analysis of nucleic acid reassociation by base pairing can be used to determine the relatedness of nucleotide sequences. This method was used to study DNA-RNA reactions (Wood et al., 1981).

The rate at which two complementary sequences reassociate depends on: (1) the concentration of cations, which decrease the intermolecular repulsion of negatively charged strands of DNA or RNA; (2) the incubation temperature, which is optimal for reassociation at about 25°C below the melting temperature of the original hybrid duplex; (3) DNA and RNA concentration, which determines the frequency of intermolecular collisions; and (4) the size of the DNA and RNA fragments.

The reaction is carried out with appropriate conditions in which the DNA and RNA are denatured by heat, allowed to reassociate and the extent of reassociation is determined by digestion with S_1 nuclease which catalyzes the hydrolysis of single-stranded DNA or RNA. After digestion to completion, the amount of nuclease resistant material is determined.

In order to do this the RNA is in large excess over the cDNA (RNA-driven reaction). To monitor the reaction the cDNA is synthesized using ^{32}P-dCTP.

$C_0t_{\frac{1}{2}}$ or $R_0t_{\frac{1}{2}}$

The C_0t or R_0t value at which half the reacting DNA or RNA is in hybrid form is termed the $C_0t_{\frac{1}{2}}$ or $R_0t_{\frac{1}{2}}$. This is characteristic of any nucleic acid. When a tracer cDNA sequence reacts with its complementary RNA sequence in excess, the reaction will spread over a R_0t of log -4 to

log 4. The R_0t values will increase with the diversity of the reacting components and the frequency at which each component is present. Rates of reaction will always depend on the ionic strength (0.3 M NaCl) and the temperature (68°C).

Examples

1. A mixture of rabbit alpha and beta globin messanger RNA of 600 nucleotides each will react with its own cDNA at 0.24 M phosphate and 68°C with a $R_0t_{\frac{1}{2}}$ of 5×10^{-3} moles/liter · sec.
2. Vitellogenin mRNA of 7100 nucleotides hybridizes to its own cDNA at a $R_0t_{\frac{1}{2}}$ of 5×10^{-3} moles/litre · sec at 0.6 M NaCl.

Calculations

Data are usually plotted on a semi-logarithmic scale as % hybridization on the y axis and log R_0t (logarithm of the product of initial concentration of the driver component in moles/litre multiplied by time of incubation in seconds, i.e. moles/litre · sec) on the x axis.

Percent hybridization is calculated from the following formula:

$$\frac{\text{(cpm in nuclease treated sample - background)}}{\text{(cpm in nuclease untreated sample - background)}} \times 100$$

The zero time or 'snap back' hybridization radioactivity is subtracted from each value.

R_0t value is calculated from the initial concentration of the driver sequence and the total time of incubation.

For example, at a concentration of 1 mg/mL, nucleic acid incubated for 1 min. will give a R_0t value of 0.2 moles/litre · sec. Similarly,

10 mg/mL and incubation for 1 hour, the R_0t value will be 120 moles/litre · sec.

The basis for the above calculation is as follows: 1 mg/mL nucleic acid represents a 0.0033 M solution of nucleotides of an average molecular weight of 300 daltons. Therefore, 1 mg/mL of nucleic acid incubated for 1 sec will give a R_0t value of 0.003 moles/litre · sec.

By using two concentrations of RNA driver the values are:

$$R_0 = 0.001 \text{ mg/mL}$$

$$R_0 = 0.1 \text{ mg/mL}$$

By varying the time of incubation at 68°C from 0 to 84 hours, log R_0t values between -3.7 and 2.0 are obtained.

Sample Calculation

1. 229E RNA driver x 229E cDNA log R_0t = 0.25

cpm GF/C filter = 40

snap back cpm = 50

total background = 90

$$\frac{\text{(cpm in nuclease treated sample - background)}}{\text{(cpm in nuclease untreated sample - background)}} \times 100$$

$$\frac{(1584 - 90)}{(1681 - 90)} \times 100 = 94\%$$